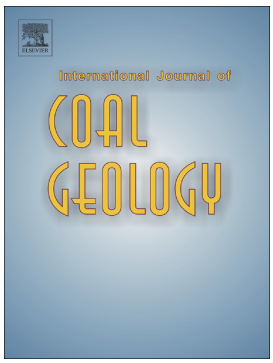

Thermal history of the Northwestern Argentina, Central Andean Basin, based on first-ever reported graptolite reflectance data

Nexxys C. Herrera Sánchez, Blanca A. Toro, Ricardo Ruiz-Monroy, Thomas Gentzis, Seare Ocubalidet, Humberto Carvajal-Ortiz

PII: S0166-5162(21)00051-3

DOI: https://doi.org/10.1016/j.coal.2021.103725

Reference: COGEL 103725

To appear in: *International Journal of Coal Geology*

Received date: 9 December 2020

Revised date: 3 March 2021

Accepted date: 7 March 2021

Please cite this article as: N.C. Herrera Sánchez, B.A. Toro, R. Ruiz-Monroy, et al., Thermal history of the Northwestern Argentina, Central Andean Basin, based on first-ever reported graptolite reflectance data, *International Journal of Coal Geology* (2021), https://doi.org/10.1016/j.coal.2021.103725

THERMAL HISTORY OF THE NORTHWESTERN ARGENTINA, CENTRAL ANDEAN BASIN, BASED ON FIRST-EVER REPORTED GRAPTOLITE REFLECTANCE DATA

Nexxys C. Herrera Sánchez[1], Blanca A. Toro[1], Ricardo Ruiz-Monroy[2], Thomas Gentzis[3], Seare Ocubalidet[3] and Humberto Carvajal-Ortiz[3]

[1]Centro de Investigaciones en Ciencias de la Tierra (CICTERRA), Universidad Nacional de Córdoba, Facultad de Ciencias Exactas, Físicas y Naturales, Consejo Nacional de Investigaciones Científicas y Tecnológicas (CONICET), Av. Vélez Sarsfield 1611, X5016CGA, Córdoba, Argentina. nexxys.herrera@unc.edu.ar; btorogr@mendoza-conicet.gob.ar

[2]Helmholtz Centre Potsdam-GFZ. German Research Centre for Geosciences, Section 3.2: Organic Geochemistry, Wissenschaftpark "Albert Einstein", Telegrafenberg, 14473, Potsdam, Germany. ricardoruizmonroy@yahoo.com

[3]Core Laboratories, 6316 Windfern Road, TX 77040, Houston, Texas, United States. thomas.gentzis@corelab.com; seare.ocubalidet@corelab.com; humberto.carvajal@corelab.com

42 pages; 9 figures; 2 tables

Corresponding author: Nexxys C. Herrera Sánchez, nexxys.herrera@unc.edu.ar

ABSTRACT. The thermal maturity from the early Paleozoic strata in Northwestern Argentina was studied using reflected light microscopy and Rock-Eval analyses. The graptolites were collected from the Acoite and Lipeón formations, from the Los Colorados section, Cordillera Oriental, and the Huaytiquina, and Muñayoc sections, Puna highland, corresponding to the "Coquena" Formation and the Cochinoca-Escaya Magmatic-Sedimentary Complex. Rock-Eval parameters were unreliable due to the low TOC, S1, and S2 values. The Cordillera Oriental region sediments have low maturity based on low reflectance (%GRo= 0.63%-1.11%) and anisotropy of graptolite. In contrast, the higher graptolite reflectance of samples from the Muñayoc and Huaytiquina sections (%GRo= 5.57%-6.62%), in the Puna region, indicates considerably higher maturity. This could result from the combination of hydrothermal fluids with a temperature range from 336 °C to 358 °C, associated volcanism, and deformation related to tectonics events which produced a higher geothermal gradient in the Puna. The Los Colorados section's thermal maturity modeling shows a better fit considering erosion episodes at the Late Paleozoic and Early Cenozoic. However, more studies about geothermal parameters and stratigraphy are necessary to corroborate these preliminary models and propose new approaches for the Puna region.

Keywords: Graptolites, Thermal Maturity, Northwestern Argentina, Ordovician, Equivalent Vitrinite Reflectance.

1. INTRODUCTION

The reflectance of bitumen, zooclasts, and vitrinite-like particles has been widely used to evaluate the thermal maturity in pre-Devonian rocks, in which primary vitrinite is absent (Kurylowicz *et al*., 1976; Goodarzi, 1984, 1985; Goodarzi and Norford, 1985, 1989; Goodarzi and Higgins, 1987; Goodarzi *et al.*, 1988; Obermayer *et al.*, 1996; Suchý *et al*., 2002; Petersen *et al*., 2013; İnan *et al.*, 2016; Luo *et al*., 2016, 2017, 2018; between others). Graptolites, conodonts, chitinozoans, and scolecodonts are commonly preserved in Early Palaeozoic rocks, and their optical properties have been widely studied (Suárez-Ruiz *et al.*, 2012; Petersen *et al*., 2013; Hartkopf-Fröder *et al.*, 2015 and references therein). Among these zooclasts, graptolites are probably the most widely used group for thermal maturity studies because of their greater abundance and wide distribution in most sedimentary lithofacies and paleoenvironments (Cole, 1994; Petersen *et al*., 2013).

Modern studies about the tubarium, the housing of planktic graptolites, confirm that it is a complexly organized organic structure produced in distinct increments called the *fuselli*. The material of the fossil graptolite tubarium consists of an aliphatic polymer and does not contain any protein, even though the structure and analysis of the housing material of modern pterobranchs indicate that it was originally collagen (Maletz *et al.*, 2016). The tubarium structure is composed of individual zooidal tubes termed the *thecae* that are interconnected through a common canal from the *sicula*, a differentiated housing from the colony founder. The two basic constructional features of the thecae are the fusellum (fusellar layer) and the *cortex* (cortical layer). Each fusellus possesses at least one oblique suture and is stacked one upon another with some lateral overlap to form a distally open tube. The cortex is secreted in distinct bandages on the surface of the thecal tubes (Maletz *et al.*, 2016: figs. 1, 4).

Graptolites were used for the first time as thermal indicators by Kurylowicz *et al*. (1976). They noted that the reflectance and optical properties of graptolite fragments in Ordovician strata of the Amadeus Basin, Australia, closely resemble those of the vitrinite. Since then, graptolites in different Ordovician, and Silurian basins, from Australia, Saudi Arabia, China, Germany, Sweden, Turkey, Canada, Poland, USA, Austria, and the Czech Republic, have been widely used for thermal maturation studies in a wide range of geological applications (metamorphic subfacies, hydrocarbon, and mineral exploration, and contact metamorphism) (Goodarzi *et al*., 1992a-b; Gentzis *et al*., 1996; Suárez-Ruiz *et al*., 2012; Hartkopf-Fröder *et al*., 2015; Weishauptová *et al*., 2017; Luo *et al*., 2016, 2017, 2018, 2020, and references therein).

The relationship between graptolite reflectance, and other thermal parameters such as equivalent vitrinite reflectance (VRo-eq), equivalent solid bitumen reflectance (BRo-eq), Rock-Eval pyrolysis Tmax, Thermal Alteration Index (TAI), and Conodont Color Alteration Index (CAI) has been established throughout the years. Goodarzi and Norford (1989) indirectly correlated the graptolite maximum reflectance with vitrinite reflectance using the CAI and described that vitrinite has a lower reflectance value than graptolite for the same CAI. Later, Petersen *et al*. (2013) determined a relationship between the random reflectance of graptolites and vitrinites through the intermediate conversion of Rock-Eval pyrolysis Tmax values, and illustrated that the graptolite random reflectance (GRo, ran) is higher than vitrinite random reflectance (VRo, ran). These authors also indicated that the maximum reflectance (Ro, max) increases gradually with burial depth. Hence, the reflectance can be used to study the burial history and maturity of Paleozoic successions. Hartkopf-Fröder *et al.* (2015) summarized the stages of oil and gas generation, and the correlation between vitrinite reflectance in coal, and optical and thermal maturity parameters including CAI,

Transmittance Color Index (TCI), Acritarch Colour Alteration Index (AAI), Spore Colour Index (SCI), Graptolite Reflectance, and Thermal Alteration Index (TAI).

Furthermore, Luo *et al.* (2018) showed that graptolite random reflectance is a better thermal maturity indicator than graptolite maximum reflectance and is more precise due to its smaller standard deviation. These authors also proposed equations to determine the thermal maturity of the graptolite-bearing sediments based on graptolite random reflectance, graptolite maximum reflectance, and solid bitumen random reflectance. Recently, Hao *et al.* (2019) used the relationship between vitrinite reflectance and graptolite reflectance proposed by Luo *et al.* (2018), and suggested a conversion equation of the equivalent vitrinite reflectance, based on Raman spectroscopy values of the graptolite tubarium structure, to assess the thermal maturity of the Early Paleozoic sequence in southwestern China. Luo *et al.* (2020) reviewed previous studies on graptolite reflectance, and presented a new equation to correlate random graptolite reflectance to equivalent vitrinite reflectance.

Studies concerning the thermal maturity of Ordovician rocks remain scarce for the Early Paleozoic sequences in the Central Andean Basin. Kley and Reinhardt (1994) used reflectance and infrared spectroscopy measurements of the organic matter to determine the organic matter maturity in Southern Bolivia. They concluded that maturity varies from very weakly diagenetic in the Subandean Ranges to low-grade metamorphic in the Eastern Cordillera.

Previous research related to geothermal studies in Northwestern Argentina was based mainly on CAI. Carlorosi *et al*. (2013) determined a 1.5- 2 CAI (*sensu* Epstein *et al*., 1977) in conodonts from the *Baltoniodus triangularis* Zone (Dp1, *sensu* Bergström *et al.*, 2009) in the Los Colorados area, Cordillera Oriental. Later, Voldman *et al*. (2017) assigned a CAI value of 3 to some specimens from the *Acodus triangularis*, *Gothodus*

vetus, and *Gothodus andinus* biozones (Tr3-Fl2). The above CAI value accounts for burial paleotemperatures ranging from 110-200 °C (*sensu* Epstein *et al*., 1977) in the Chulpios Creek, Santa Victoria area, Cordillera Oriental. Afterward, Toro *et al*. (2020) recognized conodonts of the *Baltoniodus navis* Zone with a CAI of 1.5-2 of the Epstein *et al.* (1977) scale in the Huaytiquina area Western Puna. Based on CAI and analysis of clay minerals, Do Campo *et al.* (2017) calculated the paleotemperatures for metapelites and metavolcanic rocks of the Late Cambrian-Ordovician succession in Northwestern Argentina. They concluded that there is an E-W trend ranging from diagenesis/low anchizone in the eastern flank of the Santa Victoria Range, to high anchizone/epizone in the Puna region, with intermediate values in the western flank of the Santa Victoria Range.

Graptolites from Northwestern Argentina have been studied for more than a century allowing for regional and intercontinental biostratigraphic correlations to be established (Turner, 1960; Toro 1995, 1997; Brussa *et al.*, 2008; Toro and Vento, 2013; Toro *et al*., 2015; Albanesi and Ortega, 2016; Toro and Herrera Sánchez, 2019; Herrera Sánchez *et al*., 2019) but have not been used as thermal maturity indicators up to now.

This study provides, for the first time, an early interpretation and discussion about the thermal postdepositional evolution for the Central Andean Basin in Northwestern Argentina (Fig. 1) based on graptolite reflectance, and Rock-Eval pyrolysis data.

Figure 1. Location map (size: 2-column)

2. GEOLOGICAL FRAMEWORK

The Central Andean Basin (Sempere, 1995) developed in an active margin of the western Gondwana during the Cambrian-Ordovician. It spreads over Northwestern

Argentina (NWA) and encompasses parts of Chile, Bolivia, and Perú (Astini, 2003). NWA includes, from West to East, the geomorphological provinces of Puna, Cordillera Oriental, Sierras Subandinas, and Sierras de Santa Bárbara (Fig. 1a). This study focuses on the Ordovician strata outcrops in the Puna region and the Ordovician and Early Silurian deposits exposed in the Cordillera Oriental.

The basement of the studied area is represented by the Vendian-Early Cambrian Puncoviscana Formation (Turner, 1960), which is composed mainly of a pelite-greywacke turbidite sequence. It has been affected by very low-grade metamorphism and polyphase deformation during the Early Cambrian Pampean Orogeny (Mon and Hongn, 1996; Escayola *et al*., 2011, Casquet *et al*., 2018). This unit is unconformably overlain by Middle-Late Cambrian shallow platform quartzites, sandstones, and red to greenish shales of the Mesón Group. In turn, the above group is unconformably overlain by the Late Cambrian-Early Ordovician rock succession. This unconformity is related to the rifting phase ("Irúyica Phase"; Turner and Méndez, 1975), and the eastern movement of the Arequipa-Antofalla terrain (AAt) that resulted in the opening of a V-shaped marine basin that widened northward towards Bolivia (Gohrbandt, 1992; Forsythe *et al*., 1993; Bahlburg and Hervé, 1997; Egenhoff, 2007). Alternatively, this contact has been considered as an unconformity resulting from a relative sea-level fall (Moya, 1998; Buatois *et al*., 2000; Buatois and Mángano, 2003; Mángano and Buatois, 2004) or even being a conformable depositional transition (Ruiz Huidobro, 1975; Fernández *et al*., 1982). Recently, Vaucher *et al.* (2020) recognized an episode of basin deformation around the Cambrian-Ordovician transition in NWA. These authors associated this stratigraphic unconformity to the onset of the retro-arc basin in the Cordillera Oriental, which probably occurred earlier in the western/southwestern foredeep area near the volcanic arc developed in the Puna region.

The Late Cambrian-Ordovician sedimentary sequence from the Cordillera Oriental corresponds to the Santa Victoria Group (Turner, 1964), which includes the Santa Rosita (Late Cambrian-Tremadocian), and the Acoite (Floian-Early Dapingian) formations (Astini, 2003; Buatois and Mángano, 2003; Toro *et al.*, 2015; Toro and Herrera Sánchez, 2019). In the Puna region, the fossiliferous siliciclastic marine sediments assigned to the Late Cambrian, Tremadocian, and Floian interfingering with synsedimentary lavas, and subvolcanic intrusives that were grouped into three complexes based on distinctive facies, namely the Puna Volcanic Complex, the Puna Turbidite Complex, and the Puna Shelf Complex (Zimmermann and Bahlburg, 2003; Zimmermann, 2011). On the other hand, Coira *et al.* (2004) defined the Cochinoca-Escaya Magmatic-Sedimentary Complex (CEMSC) as being composed of volcaniclastic dacites intercalated with medium- to fine-grained sandstones and massive pelites. CEMSC outcrops in the Cochinoca-Escaya, Queta, and Quichagua Ranges, eastern Puna. It is associated with volcanic breaches, hyaloclastites, cryptodomes, massive spilitized basaltic levels or padded structures, and micro-gabbros forming layers or lacolites (Coira, 2008, and references therein). The best outcrops of this complex are found in the Muñayoc section located in the Quichagua Range, Jujuy Province (Fig. 1b).

The Ordovician succession in NWA was folded by a simple structural style and was intruded by granite (Mon and Hongn, 1991). The intensity of folding increases gradually westward, from less deformed sequences such as those of the Cordillera Oriental to beds affected by intense west-verging folding with east-dipping axial plane cleavage in the Puna region (Mon and Hongn, 1991). The outcrops of Ordovician beds depicting tight folds covered unconformably by Silurian and Devonian beds were included by Mon and Hongn (1991) in the "Ocloyic Belt", with the age of deformation attributed traditionally to the "Ocloyic Phase" (Late Ordovician) (Turner and Méndez,

1975; Turner and Mon, 1979; Mon and Hong, 1991; Mon and Salfity, 1995, between others). This intra-Ordovician deformation has been documented in several outcrops of Early Ordovician rocks in the transition between Puna and the Cordillera Oriental as well as in the Salar del Rincón area, western Puna (Bahlburg, 1990; Bahlburg and Hervé, 1997; Moya, 1999; Astini, 2003; Hongn and Vaccari, 2008). On the other hand, Moya (1999, 2003, 2015) discussed the conceptual framework in which the "Ocloyic Phase" was defined. This author proposed that the Paleozoic deposits were only subject to block tectonics and later folded together with Cretaceous deposits as a result of the Andean Orogeny. The lack of evidence of an angular unconformity separating the Late Ordovician deposits outcropping in the Argentine Cordillera Oriental from the overlying Early Paleozoic sequences supports the interpretation of this author. Besides, K-Ar ages of fine-grained micas obtained for Ordovician very low-grade metapelites of the Bolivian Cordillera Oriental do not show the existence of an orogenic activity during the Late Ordovician. Therefore, the deformation was attributed to either a Late Devonian-Early Carboniferous event (Kley and Reinhardt, 1994; Tawackoli *et al*., 1996) or to a Late Carboniferous-Early Permian orogenic episode (Jacobshagen *et al*., 2002). Astini (2002) considered that the "Ocloyic Phase" comprises a combination of eustatic decay due to the rapid growth phase of the Gondwanic ice sheet and subordinate tectonics.

During the Silurian-Devonian times, the different southwestern Gondwana basins were generally grouped as underfilled shallow marine basins (Starck, 1995 and references therein). At NWA, and southern Bolivia, approximately 3000 m of siliciclastic rocks were deposited between the Ludlowian-Frasnian (57 My) (Dalenz-Farjat *et al.*, 2002). At the beginning of the Carboniferous, another diastrophic event occurred in NWA. It was probably related to a minor reorganization of the Chilenian

Terrain edge relative to Gondwana, referred to as the "Chanic Phase" (Starck, 1995). Ramos *et al.* (1984) interpreted this phase as a collisional event in plate tectonics terms. Although this orogeny was not intense in the study area, the diastrophism, and hiatus represent the onset of a new tectonostratigraphic cycle, and formation of the Tarija Basin, in the south of Bolivia, and Sierras Subandinas belt at NWA, which is considered as an intracratonic basin with a low subsidence rate (Starck *et al.*, 2002). It is probable that a large part of the Cordillera Oriental remained emerged at this time, which would explain the scarce Siluro-Devonian deposits and also the erosional truncation of the Santa Victoria Group (Starck, 1995). The Carboniferous deposits from NWA are separated from the Devonian succession by a major unconformity related to the "Chanic Phase" (Starck *et al.* 1992, 1993 and references therein), resulting in a hiatus of approximately 50 My (Starck, 1995).

In the Tarija Basin, the Carboniferous-Jurassic interval is characterized by various depositional sequences. The base of the succession overlies a major regional unconformity that is locally modified by deep erosion. This unconformity is most pronounced in the southwestern part of the area where the Silurian-Devonian section in parts of the Cordillera Oriental is completely eroded (Starck, 1995: fig. 6). A network of deeply eroded paleovalleys is deposited on this regional unconformity, incising different levels of the Devonian rocks (Starck *et al.*, 1992, 1993). In the Early Jurassic, a new event resulted in a widespread unconformity and marked a change in regional stress fields. In NWA, an important change in the style of subsidence occurred with the Late Jurassic "Araucanian Phase", which effectively concluded with the development of the Tarija Basin. The extension dissected the old epeiric basin into a suite of fault-controlled half-grabens. Here, the Cretaceous-Paleogene Salta Group developed as a rift basin fill (Starck, 1995, 2011 and references therein).

2.1 Argentine Cordillera Oriental

The Cordillera Oriental is a high relief "thick-skinned type" thrust system with dominant east vergence, in which the Acoite Formation consists of thick, upward-shallowing beds related to a storm-dominated deltaic system (Astini, 2003; Waisfeld and Astini, 2003). The Los Colorados area is located approximately 23˚ 33' S, and 65˚ 40' W in the Jujuy Province (Fig. 1b). The stratigraphy appears to be complete, but most of the described units are separated by stratigraphic discontinuities, such as relative fall surfaces, subaerial exposure, transgressive episodes, or coplanar surfaces. However, these surfaces do not always have an obvious expression from a stratigraphic perspective (Astini *et al.*, 2004). In this area, the Acoite Formation reaches a maximum thickness of almost 2300 m (Waisfeld *et al.*, 2003; Astini *et al.*, 2004; Toro and Herrera Sánchez, 2019) (Fig. 2). It is composed mainly of greenish-gray shale and fine-sandstone, alternating with dark-gray, and black shale, and siltstone deposited in a middle to distal shelf setting (Waisfeld *et al.*, 2003) during the Early Ordovician (*Tetragraptus phyllograptoides*, *T. akzharensis*, *Baltograptus* cf. *B. deflexus*, and *Didymograptellus bifidus* biozones). The upper part of the unit, in which the *Azygograptus lapworthi* Biozone (Middle Ordovician) has been recently recognized in the western side of the Cordillera Oriental by Toro and Herrera Sánchez (2019), is a massive, highly bioturbated sandy facies that developed abruptly, overlying an upward-thickening mesoscale cycle with tidal influence (Astini, 2003; Waisfeld and Astini, 2003). Few meters above these levels, a short interval composed of purplish shales with heterolytic intervals and pale red sandstone with abundant cross-bedded strata (Astini, 2003) is assigned to the Alto del Cóndor Formation (43 m thick) (Astini *et al.*, 2004) (Fig. 2). Carlorosi *et al.* (2013) assigned a short transgressive interval that produces conodonts from the *Baltoniodus triangularis* Zone (Early Dapingian, Dp1) to the Lower

Member of this unit. The overlain Sepulturas Formation (63.5 m thick) (Fig. 2) has a largely coarsening upward arrangement with a variety of open-marine fauna (Astini, 2003). Above it, a regionally extended pebbly-sandy mudstone (Moya and Monteros, 1999) truncates the earlier stratigraphy. This diamictite is known as the Zapla Formation (20 m thick) (Fig. 2) and is relatively well accepted to be of glacial origin, constrained to the uppermost Ordovician, and hence, correlated with the Late Ordovician ice age (Astini, 1999, 2002). The Ordovician succession appears to be in paraconformity with the overlain Silurian deposits (Astini *et al.*, 2004). In the Cordillera Oriental, Early Silurian graptolites (*Stimulograptus sedgwickii*, *Clinoclimacograptus retroversus*, and *Paraclimacograptus innotatus*) were recovered from the overlying strata corresponding to the Lipeón Formation (100 m thick) (Fig. 2) (Toro, 1995), which seem to record an open-shelf environment formed by postglacial transgression (Astini, 2003). Above this unit, the Silurian-Early Devonian deposits of the Arroyo Colorado Formation (Grahn and Gutiérrez, 2001; Aparicio González *et al.*, 2020), reaching 27.5 m in thickness, are constituted by purple-gray muddy, and mottled massive sandstone with good banding development that reflects variable intensities of bioturbation rates (Astini *et al.*, 2004) (Fig. 2). The Paleozoic sequence underlies, by an angular unconformity, the Cretaceous deposits of the Pirgua Subgroup (base of the Salta Group), which represents, in general, ~700 m of a continental sedimentation cycle of red-purple clastic facies. The Pirgua Sg. starts with fluvial facies interdigitating with alluvial-eolian facies in the Tres Cruces subbasin (Fig. 1b) (Boll and Hernández, 1986; Marquillas *et al.*, 2005). It represents the entire *syn-rift* state of the basin infilling, intimately related to direct faults, restricted to distensive grabens, and hemigrabens (Starck, 2011). The *pre-rift* successions were eroded from the rift margins as a result of rift flank uplift. The *post-rift* records two subgroups: the Balbuena Sg., and the Santa Bárbara Sg. The Yacoraite Formation

(Cretaceous-Paleogene; *sensu* Marquillas *et al.*, 2005) included in the Balbuena Sg., mainly consists of 315 m thick of carbonatic rocks exposed in the Espinazo del Diablo (Tres Cruces Basin) which is related to the second Cretaceous marine ingression (Astini *et al.*, 2019).

Figure 2. Stratigraphic column from the Los Colorados area (size: 1.5-column)

2.2 Argentine Puna

The Puna morpho-structural province is a plateau with average highs above 3500 m. The Early Paleozoic is represented by sedimentary deposits and associated volcanism. It is widely accepted that the region comprises two submeridional belts, corresponding to the western and eastern, which were developed from a Cambrian rift margin to a Floian back-arc until a Darriwilian turbidite sequence in a foreland basin system (Astini, 2003, 2008 and references therein).

In the Huaytiquina section located in the western belt of the Argentine Puna (Fig. 1b), the oldest deposits (900 m thick) correspond to the Aguada de la Perdíz Formation (Puna Volcanic Complex *sensu* Zimmermann, 2011) which is composed of volcanic andesitic breaches, andesitic lava flows, and riolitic-andesitic pyrocalstics (Monteros *et al.*, 1996) (Fig. 3a). More recently, Toro and Herrera Sánchez (2019) and Toro *et al.* (2020) recognized the presence of the *Azygograptus lapworthi* (Dp1) and "*Isograptus victoriae*" (Dp2) biozones, in the middle part of this section, by the occurrence of key graptolites, and conodonts in deposits corresponding to the "Coquena" Formation (Puna Turbidite Complex *sensu* Zimmermann, 2011) (1450 m thick) (Fig. 3a). This unit is unconformably overlain by the Balbuena Sg. (Yacoraite Formation), which, in turn, is unconformably covered by Cenozoic red sandstones with intercalated shales (Monteros *et al.*, 1996). The paleogeographic analysis of the Salta Group (Salfity and Marquillas, 1994) shows that during the start of the accumulation in

the western Puna, a positive structure -Alto de Huaytiquina- was located to the west of the Sey subbasin. For this reason, the *syn-rift* deposits of the Pirgua Sg. were not accumulated. That structure was overflooded in the *post-rift* stage, allowing the Balbuena, and Santa Barbara subgroups to accumulate on the Paleozoic basement and extend towards the Chilenian Terrain (Marquillas and Matthews, 1996). The stratigraphic framework in the area ends with the Cenozoic volcanic and Quaternary deposits (Monteros *et al.*, 1996).

In the Muñayoc section, eastern Puna (Fig. 1b), Toro and Herrera Sánchez (2019) and Lo Valvo *et al.* (2020: fig. 2) recognized four graptolite biozones (*T. akzharensis*, *B.* cf. *B. deflexus*, *D. bifidus*, and *A. lapworthi*) in deposits corresponding to the CEMSC (*sensu* Coira *et al.*, 2004). The stratigraphic sequence reaching 153 m thick overlies the peperites representative of the Ordovician submarine volcanism (Coira *et al.*, 2004) (Fig. 3b). At the top of this section, an angular unconformity separates the CEMSC from deposits of the Balbuena Sg. (Starck, 2011: fig. 2).

A high-resolution correlation of the mentioned localities from the Puna region with the classical localities from the western flank of the Argentine Cordillera Oriental was recently proposed based on graptolite-conodont biostratigraphic analysis (Toro and Herrera Sánchez, 2019; Herrera Sánchez *et al.*, 2019; Toro *et al.*, 2020).

Figure 3. Stratigraphic sections from the Argentine Puna (size: 1.5-column)

3. SAMPLING AND METHODS

3.1 Samples

A total of 14 samples were collected from Northwestern Argentina, with seven samples from the Los Colorados area (Fig. 1b), the Cordillera Oriental, corresponding to the Acoite, and Lipeón formations (Fig. 2). Another seven samples were collected

from the Huaytiquina and Muñayoc areas (Fig. 1b) in the Puna highland and were previously assigned to the "Coquena" Formation (Fig. 3a) and the CEMSC (Fig. 3b), respectively. For identifying the graptolite taxa listed in Figure 4, the reviewed taxonomy presented in the *Treatise of Invertebrate Paleontology* (Maletz *et al.*, 2018a-b) was used. The biostratigraphic discussions are based on the Ordovician graptolite framework successively proposed by Toro (1994, 1997), Toro and Maletz (2007), Toro and Vento (2013), Toro *et al.* (2015), Toro and Herrera Sánchez (2019), and recently summarized by Herrera Sánchez *et al.* (2019) and Toro *et al.* (2020). The proposal of Bergström *et al.* (2009) for referring to the graptolite ages, regional correlations, and global stages was followed.

Figure 4. Table with the provenance and taxonomy of the graptolite samples (size: 2-column)

3.2 Rock-Eval analysis

For the Rock-Eval pyrolysis/TOC analysis, the Rock-Eval 7S instrument was used to determine the parameters shown in Table 1. The analysis was performed using the Basic/Bulk-Rock method (full cycle of pyrolysis and oxidation). The standard used was IFP 160000. Approximately 60 mg of sample powder were placed inside crucibles. The samples were pyrolyzed to measure the contained hydrocarbons as well as CO_2 and CO via a flame ionization detector (FID), and IR cells, respectively. The pyrolysis temperature was initiated at 300 °C isothermal for 3 minutes and increased gradually at a rate of 25 °C/min until 650 °C. For determining the oxidized mineral carbon, and residual carbon, the oxidation oven temperature was 300 °C isothermal for 30 s, and increased gradually by 25 °C/min until 850 °C, and held for 5 min at 850 °C.

3.3 Microscopy

Samples were prepared under the standard method (ISO 7404-2, 2009). The graptolite random reflectance (%GRo) was determined under plane-polarized light using a Zeiss Axio Imager A2m reflected light microscope equipped with a photometer, following ISO 7404-5 (2009) and ASTM D7708-14 (2014) methods. The equivalent vitrinite reflectance (%VRo-eq) was calculated from the mean random graptolite reflectance using the equation established by Petersen *et al.* (2013) (%VRo-eq= [GRo*0.73] +0.16). The paleotemperature "Peak Temperature" (Tpeak) was calculated under "normal" geothermal gradient conditions (Tpeak= [lnVRo-eq+1.68]/0.0124), and hydrothermal conditions (Tpeak-hy= [lnVRo-eq+ 1.19]/0.0782) following Barker and Pawlewicz (1994), and Hartkopf-Fröder *et al.* (2015). Graptolites were identified by their granular or non-granular texture (Goodarzi, 1984; Goodarzi and Norford, 1987) and morphology (Teichmüller, 1978).

All the measurements of the Rock-Eval analysis, graptolite Ro, vitrinite Ro-eq, and calculated paleotemperatures are shown in Tables 1 and 2. The Tpeak values shown in Table 2 are associated with CAI values taken from the literature (Carlorosi *et al.*, 2013; Toro *et al.*, 2020).

3.4 Basin Modeling

To test the results about the burial and thermal history of the Central Andean Basin, based on the graptolite reflectance data for Northwestern Argentina, the PetroMod 1D Express Basin Modeling (from IES GmbH, Schlumberger) was used. For this modeling, the geodynamical approaches explained in the geological framework of this work were considered. The PetroMod software runs numerical simulations involving parameters from each stratigraphic interval such as thickness, lithology, and age, defined depositional and erosional events, and fixing paleowater depth (PWD), seawater interface temperature (SWI), and heat flow (HF) values. Variations in sea

water depth over time could be assumed to be irrelevant because thermal evolution is mainly affected by sediment thickness rather than the depth of the water; SWI is ~21.44 °C. The HF trend was estimated from the typical values associated with different types of sedimentary basins summarized by Allen and Allen (2005: fig. 9.39). Besides, the regional assumptions of Ege *et al.* (2007), and Moretti *et al.* (1996) for the Cenozoic and current values were considered. The specific heat flows used are: Ordovician retro-arc basin (477 My), 70 mW/m^2; collisional event-"Chanic Phase" (359 My), 70 mW/m^2; Cretaceous *rift* event (130 My), 90 mW/m^2; *post-rift* event (60 My), 65 mW/m^2; Early Oligocene exhumation (30 My), 55mW/m^2; at present-day (0 My), 65 mW/m^2. The thickness of the Pirgua, and Balbuena Sg. (Yacoraite Formation) were taken from the Tres Cruces section (Rubiolo *et al.*, 2003; Marquillas *et al.*, 2005).

4. RESULTS AND DISCUSSION

4.1 Rock-Eval pyrolysis, and Total Organic Carbon (TOC)

Rock-Eval/pyrolysis and TOC data for the sections are shown in Table 1. TOC content was very low, ranging from 0.15 to 0.50 wt% in the suite from the Cordillera Oriental, and from 0.09 to 0.90 wt% in the suite from Puna. The S1 values were less than 1.0 mg HC/g rock, except for sample LC-10+12 m (1.88). The S2 values were also very low (<0.36 mg HC/g rock), except for sample LC-10+12 m (1.30). As a result of the very low S2 values, the Tmax values are unreliable and should be discarded. The same applies to the calculated parameters, such as HI, OI, and PI. Rock-Eval pyrolysis data will not be discussed further. The level of thermal maturity was determined by measuring the graptolite reflectance, as will be discussed later.

It is interesting to note that the large difference in thermal maturity between samples retrieved from the LC and MU groups masks their differences in TOC. With an

average of 0.74 wt% the TOC of the samples from MU is nearly three times larger than the TOC of samples in the LC group whose TOC is on average 0.28 wt%. This might reflect a higher amount of deposited organic matter or/and its better preservation in the depositional setting where samples of MU were deposited compared to samples collected in LC.

Table 1. Rock-Eval pyrolysis results

4.2 Age and optical characteristics of the graptolites

The graptolite-bearing samples were collected from three outcropping sections in which the *Tetragraptus akzharensis*, *Baltograptus* cf. *B. deflexus*, *Didymograptellus bifidus*, *Azygograptus lapworthi*, and "*Isograptus victoriae*" biozones were developed (Figs. 2-3), indicating an Early Floian (Fl1) to Early Dapingian (Dp2) age. Besides, the samples that originated from the Lipeón Formation were assigned to the *Stimulograptus sedgwickii* Biozone, which indicates an Aeronian (Early Silurian) age (Toro, 1995) (Fig. 2). The recognized graptolite taxa are listed in Figure 4, which also includes the provenance of the samples.

The graptolite fragments were identified based on morphological features such as the tubarium structure (Figs. 5a-d), common canal, thecae, and thecal branching (Fig. 6c; Figs. 7e-f). The structure corresponds to fine bright and dark lamellar layers on the fusellar tissue (Figs. 5e-f). The graptolites from the Puna region, which are preserved in shales (Muñayoc section; *sensu* Martínez *et al.*, 1999) and calcareous sandstones (Huaytiquina section; *sensu* Toro *et al.*, 2020) are non-granular (Figs. 5a-f; Figs. 6a-f; Fig. 7a). On the other hand, the zooclast fragments from the Los Colorados section, Cordillera Oriental, were poorly preserved and fragmented, and were encountered mostly normal to the bedding plane, and had a pitted texture (Figs. 7b-d).

The lower reflectance and weaker anisotropy of graptolites from the Cordillera Oriental region (Table 2) indicate their low maturity. On the other hand, the graptolite fragments from the Muñayoc, and Huaytiquina sections in Puna are high-reflecting, pointing to considerably higher maturity.

Table 2. Graptolite, and equivalent vitrinite reflectance, Tpeak

Figures 5, 6, and 7. Graptolites under reflected light (size: 2-column each one)

4.3 Graptolite reflectance and thermal maturity of Paleozoic rocks from Northwestern Argentina

Graptolite random reflectance measurements from the Los Colorados section range from 0.63%-1.11% (Table 2) with corresponding VRo-eq between 0.62% to 0.97% (Table 2), indicating that the organic matter is between the early to the peak stages of the oil window, corresponding to the catagenetic stage (*sensu* Abad, 2007). The reflectance histograms of the six samples analyzed from the above section are displayed in Figure 8 (a-f). The calculated Tpeak values in the range of 97 °C-133 °C reflect the maximum burial depth experienced by the graptolites in this section and agree with the temperature estimated from the 1.5-2 CAI of conodonts from the Lower Member of the Alto del Cóndor Formation (Carlorosi *et al.*, 2013), which is approximately 100 °C. One sample (LC-10+12 m) did not contain any measurable graptolite fragments. The eastern basin, which coincides with the present-day Cordillera Oriental, did not experience synsedimentary magmatic activity, so the thermal parameters measured in this work could indicate the maximum depth of burial. The three higher Tpeak values (119, 122, and 133 °C) corresponding to the graptolites in samples LC-17, LC-21, and LC-24+40m could reflect some influence of hydrothermal activity.

Figure 8. Histograms (size: 2-columns)

On the other hand, the graptolite random reflectance in the Argentine Puna region is 6.15% in the Huaytiquina section and varies between 5.57%-6.62% in the Muñayoc area (Table 2). The equivalent vitrinite reflectance in the Argentine Puna ranges from 4.23%-4.99% (Table 2), and Tpeak varies from 252 °C to 265 °C, indicating post-mature organic matter (dry gas stage) and consistent with an epizone metapellitic zone (*sensu* Abad, 2007). Furthermore, graptolite fragments having considerably higher reflectance, from 8.8-10.1%, were measured (Table 2), corresponding to VRo-eq of 6.5-7.5%, and temperatures above 300 °C. These graptolites exhibited strain anisotropy, although the fusinal layer structure was still visible when the analyzer was inserted (Fig. 5f). These very high %Ro values of graptolites affected by tectonic activity were not used to model the level of thermal maturity in the Puna region.

The common occurrence of kaolinite in the slates of the Cochinoca-Escaya Range in the Puna region, coupled with the substitution of chlorite by interstratified lower-temperature phases in most of these rocks, and the occurrence of jarosite in a metadacite indicate the presence of hydrothermal fluids with high H^+/cation ratios. These fluids can produce acid-type alteration at temperatures between 100 °C and ~300 °C (Do Campo *et al.*, 2017). Besides, the Ordovician rocks in this study are related to mineralized quartz veins, gold-bearing "saddle reefs" with As, Fe, Cu, Pb, Zn, Sb sulfides, and sulfosalts of silver in the Cochinoca-Escaya, and Rinconada ranges (Craig *et al.*, 1995; Coira *et al.*, 2001). Likewise, Coira *et al.* (2004) recognized concentrations of pyrite crystals with the development of pressure forms filled with neoformed phyllosilicates, probably the product of hydrothermal alteration, in the pelitic facies of the CEMSC.

For these reasons, the data presented in this work provides an estimate of the temperature of the hydrothermal fluids, which ranges from 336 °C to 358 °C in the Puna region (Table 2). Such values are close to the maximum temperatures estimated by Do Campo *et al.* (2017), which explains the highest measured random reflectance values measured on three graptolite tubaria collected at the Puna region (%GRo~10-11%). The above temperatures are so high that they are beyond dry gas (methane) generation or retention. The strain anisotropy exhibited by the graptolites in this region (Figs. 5e-f) is characteristic of organic matter found in orogenic belts that have experienced tectonic deformation such as thrusting and folding (Goodarzi and Norrord, 1985). The "Ocloyic Phase" and Central Andes uplift had a considerable impact on the very high reflectance and strain anisotropy attained by the graptolites collected from the Argentine Puna. Besides, in the present-day Puna region, the deposits assigned to Tremadocian-Dapingian ages contain abundant intercalated volcaniclastics rocks (Bahlburg, 1990; Zimmermann and Balhburg, 2003; Zimmermann, 2011), which points to intense magmatic activity during deposition (Mon and Salfity, 1995). The very high thermal maturity of the graptolites in the Puna region could be explained by combined effect of higher geothermal gradients associated with the synsedimentary volcanism, hydrothermal fluids, as well as tectonism, i.e., during the Ocloyic Orogeny, and Central Andes uplift.

The 1.5-2 CAI value of conodonts from the Huaytiquina section (Toro *et al.*, 2020), which correspond to ~100 °C of the Epstein *et al.* (1977) table, does not coincide with the paleotemperature obtained from the reflectance measurements (i.e., sample RH-A, Table 2) that indicate temperatures greater than 300 °C. This is most likely due to the thermal effect of hydrothermal fluids on the graptolite organic matter, which is more sensitive to temperatures than fluorapatite, especially in overmatured sediments

(Goodarzi and Norford, 1985). The temperatures of 300 ^{o}C are in agreement with those estimated by the CAI values of 4-5 of the conodonts in the Salar del Rincón area in southern Puna (Do Campo *et al.*, 2017). However, the correlation between graptolite reflectance and CAI values greater than 4-5 is not clear (Goodarzi and Norford, 1985; Goodarzi *et al.*, 1992; Luo *et al.*, 2020) and should be treated with caution.

As a consequence of the hydrothermal effect associated with volcanism (Astini, 2003; Zimmermann and Bahlburg, 2003; Coira *et al.*, 2004; Zimmermann, 2011; Do Campo *et al.*, 2017 and references therein), the graptolite reflectance, and accordingly the equivalent vitrinite reflectance do not indicate the maximum depth of burial of the "Coquena" Formation, and CEMSC strata in the Argentine Puna region north of 24^{o} S latitude.

4.4 Thermal maturity modeling: preliminary comments

Several thermal models were carried out with PetroMod to test the thermal conditions for the Central Andean Basin only at the Los Colorados section, Cordillera Oriental, because other studied sections from the Puna region are probably altered by hydrothermal fluids and volcanic intrusives. The thermal evolution of the basin was reconstructed under five different conditions (Fig. 9): a) considering a complete Cretaceous and Cenozoic succession overlying the Paleozoic sequence taken as reference the thickness of the Tres Cruces section (>3500 m); b) considering that during 358-130 My, after the "Chanic Phase", a thickness of ~3000 m were deposited in Los Colorados area as occurred in the Sierras Subandinas belt (*sensu* Starck, 1995); c) considering that is probably that the Argentine Cordillera Oriental was emerged between 358-130 My, and ~900 m were eroded after the "Chanic Phase"; d) considering that ~265 m were eroded since 38 My until now as a product of the Central Andes uplift; e) considering c, and d in the same input data.

As shown in Figure 9a, vitrinite reflectance at the middle part of the Acoite Formation (at ~8500 m depth) considering a complete Cretaceous and Cenozoic succession overlying the Paleozoic sequence is about 4.55%. This high trending in VRo also occurs when a thickness of ~3000 m deposited between 358-130 My was considered. In this case, vitrinite reflectance measurement is 4.55% at ~7500 m depth (Fig. 9b). In both models, reflectance values exceed the obtained VRo-eq in this work (Table 2). On the other hand, in the alternative where ~900 m were eroded between 358-130 My, vitrinite reflectance is 1.10% at ~2200 m depth (Fig. 9c). Meanwhile, when a thickness of ~265 m was eroded during the Central Andes uplift in the latest 38 My, VRo at the middle part of the Acoite Formation is about 1.40% at ~2200 m depth (Fig. 9d). The latest alternative is considering options c and d in the same input data. In this case, vitrinite reflectance is 0.97% at ~2200 m depth (Fig. 9e). This approach considering erosion episodes at the Late Paleozoic and Early Cenozoic seems to fit with the geothermal parameters (VRo-eq) measured in this work (Table 2), which ranges between 0.80%-1.00% at the middle part of the Acoite Formation, and could explain the evolution of the Los Colorados section. This model agrees with the hypothesis that part of the Argentine Cordillera Oriental remains emerged between the Late Devonian and Early Cretaceous, which explain the scarce Siluro-Devonian strata (Starck, 1995). The deposits eroded at this time (~900 m) would probably be part of the Cinco Picachos Supersequence (Zapla, Lipeón, Baritú=Arroyo Colorado, and Porongal formations) that reaches more than 2000 m thick in the Cinco Picachos Range along the boundary between the Cordillera Oriental, and Sierras Subandinas belt (*sensu* Starck, 1995). On the other hand, also it is probably that the Los Colorados area was an emerged zone since 38 My when the Cordillera Oriental started to uplift as a consequence of the development of the Central Andes (*sensu* Coutand *et al.*, 2001), producing the erosion

of ~265 m of the Yacoraite Formation until now. However, more studies about geothermal parameters and stratigraphy for Northwestern Argentina are necessary to corroborate these preliminary models, and propose new approaches for the Puna region.

Figure 9. Thermal maturity modeling (size: 2-column)

5. CONCLUSIONS

Graptolite reflectance can be used to determine the level of maturity of organic matter, but other factors such as hydrothermal fluid activity, magmatism, and tectonism can alter the results and the interpretations.

The VRo-eq values calculated from the mean random reflectance of the graptolites from the Los Colorados section, Cordillera Oriental, range from 0.62%-0.97% with corresponding Tpeaks of 97°C and 133°C. These values place the organic matter in the oil window (early to middle part) and reflect the shallow burial depth of the graptolite-bearing interval in this area of the Central Andean Basin.

The high graptolite reflectance values from the Puna region between 5.57%-6.62% and corresponding VRo-eq between 4.23%-4.99% place the organic matter in the post-mature stage (even beyond dry methane gas generation/presentation). Such a high maturity could be the result of the combined effects of hydrothermal fluids, higher geothermal gradient associated with volcaniclastics, and deformation from tectonics events. The latter resulted in the high strain anisotropy of the graptolites.

The results presented in this work are in agreement with the trend proposed by Do Campo *et al.* (2017), which reflects higher temperatures (high anchizone/epizone) in the Puna region than those obtained for the Cordillera Oriental (catagenesis/low anchizone). It is also coincident with the proposed location of the Ocloyic deformation belt.

Modeling considering erosion episodes at Late Paleozoic and Early Cenozoic seems to fit with the geothermal parameters (VRo-eq) measured in this work, which ranges between 0.80%-1.00% at the middle part of the Acoite Formation, and could explain the evolution of the Los Colorados section. However, more studies about geothermal parameters and stratigraphy are necessary to corroborate these preliminary models, and propose new approaches for the Puna region.

ACKNOWLEDGEMENTS

We would like to thank the editor, Prof. Deolinda Flores, for her expedient and professional manner she handled our manuscript and the two anonymous reviewers for offering valuable comments and suggestions, which resulted in the improvement of the manuscript. N.C.H.S. thanks to M. Ezpeleta for providing information about the software to reproduce the thermal maturity model. This work was supported by the Agencia Nacional de Promoción Científica y Tecnológica (PICT 2016-0558), and Consejo Nacional de Investigaciones Científicas y Técnicas (CONICET). It is a contribution to 653 IUGS-IGCP project -The onset of the Great Ordovician Biodiversification event-, and was developed on the framework of the Ph.D. thesis of the first author (N.C.H.S).

REFERENCES

Abad, I., 2007. Physical meaning and applications of the illite Kübler index: measuring reaction progress in low-grade metamorphism, in: Nieto, F., Jiménez-Millán, J. (Eds.), Diagenesis and low-Temperature Metamorphism, Theory, Methods and Regional Aspects. Sociedad Española: Sociedad Española Mineralogía, pp. 53–64.

Albanesi, G.L., Ortega, G.C., 2016. Conodont and graptolite biostratigraphy of the Ordovician System of Argentina, in: Montenari, M. (Ed.), Stratigraphy & Timescales. Oxford: Elsevier Inc, pp. 61–121.

Allen, P.A., Allen, J.R., 2005. Basin analysis: Principles and Applications. Blackwell Scientific Publications, Oxford.

Aparicio González, P., Uriz, N., Arnol, J., Martínez Dopico, C., Cayo, L.E., Cingolani, C., Impiccini, A., Stipp Basei, M.A., 2020. Sedimentary provenance analysis of the ordovician to devonian siliciclastic units of the Subandean Ranges and Santa Barbara System, northwestern Argentina. Journal of South American Earth Sciences, https://doi.org/10.1016/j.jsames.2020.102629

ASTM Standard D7708-14., 2014. Standard Test Method for Microscopical Determination of the 593 Reflectance of Vitrinite Dispersed in Sedimentary Rocks. ASTM International, West 594 Conshohocken, PA.

Astini, R.A., 1999. Sedimentary record, volcano-tectonic cyclicity and progressive emergence of an Early Ordovician perigondwanic volcanic arc: The Famatinian System, in: Fraft, P., Fatka, O. (Eds.), Quo vadis Ordovician?. Acta-Universitatis Carolinae Geologica (1-2), pp. 115–118.

Astini, R.A., 2002. Los conglomerados basales del Ordovícico de Ponón Trehue (Mendoza) y su significado en la historia sedimentaria del terreno exótico de Precordillera. Revista de la Asociación Geológica Argentina 57, 19–34.

Astini, R.A., 2003. Ordovician Basins of Argentina, in: Benedetto, J.L. (Ed.), Ordovician fossils of Argentina. Secretaría de Ciencia y Tecnología, Universidad Nacional de Córdoba, pp. 1–74.

Astini, R.A., 2008. Sedimentación, facies discordancias y evolución paleoambiental durante el Cambro–Ordovícico, in: Coira, B., Zappetteni, E.O. (Eds.). Geología y

recursos naturales de la provincia de Jujuy, Relatorio del 17° Congreso Geológico Argentino, Buenos Aires: Asociación Geológica Argentina, pp. 50–73.

Astini, R.A., Waisfeld, B.G., Toro, B.A., Benedetto, J.L., 2004. El Paleozoico inferior y medio de la región de Los Colorados, borde occidental de la Cordillera Oriental (Provincia de Jujuy). Revista de la Asociación Geológica Argentina 59, 243–260.

Astini, R.A., Coppa Vigliocco, A., Gómez, F.J., 2019. Una cuña marina dominada por mareas en la base de la Formación Lecho en el extremo noroeste argentino. Revista de la Asociación Geológica Argentina 77 (2), 271–295.

Bahlburg, H., 1990. The Ordovician basin in the Puna of NW Argentina and N Chile: geodynamic evolution from back-arc to foreland basin. Geotektonische Forschungen 75, 1–107.

Bahlburg, H., Hervé, F., 1997. Geodynamic evolution and tectonostratigraphic terranes of northwestern Argentina and northern Chile. GSA Bulletin 109 (7), 869–884.

Barker, C.E., Pawlewicz, M.J., 1994. Calculation of vitrinite reflectance from thermal histories and peak temperatures. A comparison of methods, in: Mukhopadhyay, P. K., Dow, W.G. (Eds.), Vitrinite Reflectance as a Maturity Parameter: Applications and Limitations. ACS Symposium Series 570, pp. 216–229.

Bergström, S.M., Chen, X., Gutiérrez-Marco, J.C., Dronov, A., 2009. The new chronostratigraphic classification of the Ordovician System and its relations to major regional series and stages to δ13C chemostratigraphy. Lethaia 42 (1), 97–107.

Boll, A., Hernandez, M., 1986. Interpretación estructural del área de Tres Cruces. Boletín de Informaciones Petroleras, Tercera Época, Año III, 7, 2–14.

Brussa, E.D., Toro, B.A., Vaccari, N.E., 2008. Bioestratigrafía del Paleozoico inferior en el ámbito de la Puna, in: Coira, B., Zappetteni, E.O. (Eds.), Geología y recursos

naturales de la provincia de Jujuy, Relatorio del 17° Congreso Geológico Argentino, Buenos Aires: Asociación Geológica Argentina, pp. 93–97.

Buatois, L.A., Mángano, M.G., Moya, M.C., 2000. Incisión de valles estuarinos en el Cámbrico Tardío del noroeste argentino y la problemática del límite entre los grupos Mesón y Santa Victoria. Segundo Congreso Latinoamericano de Sedimentología, Resúmenes, 55.

Buatois, L.A., Mángano, M.G., 2003. Sedimentary facies, depositional evolution of the Upper Cambrian - Lower Ordovician Santa Rosita formation in northwest Argentina. Journal of South American Earth Sciences 16, 343–363.

Carlorosi, J., Heredia, S., Aceñolaza, G., 2013. Middle Ordovician (Early Dapingian) conodonts in the Central Andean Basin of NW Argentina. Alcheringa 37 (3), 299–311.

Casquet, C., Dahlquist, J.A., Verdecchia, S.O., Baldo, E.G., Galindo, C., Rapela, C.W., Pankhurst, R.J., Morales, M.M., Murra, J.A., Mark Fanning, C., 2018. Review of the Cambrian Pampean orogeny of Argentina; a displaced orogen formerly attached to the Saldania Belt of South Africa?, Earth-Science Reviews 177, 209–225.

Coira, B., 2008. Volcanismo del Paleozoico inferior en la Puna Jujeña, in: Coira, B., Zappetteni, E.O. (Eds.), Geología y recursos naturales de la provincia de Jujuy, Relatorio del 17° Congreso Geológico Argentino, Buenos Aires: Asociación Geológica Argentina, pp. 267–292.

Coira, B., Caffe, P.J., Ramírez, A., Chayle, W., Díaz, A., Rosas, S., Pérez, A., Pérez, E.M.B., Orozco, O., Martínez, M., 2001. Hoja Geológica 2366-I/2166-III "Mina Pirquitas", Provincia de Jujuy. Servicio Geológico Minero Argentino, Instituto de Geología y Recursos Minerales, Boletín 269.

Coira, B., Caffe, P.J., Ramírez, A., Chayle, W., Díaz, A., Rosas, S., Pérez, A., Pérez, E.M.B., Orozco, O., Martínez, M., 2004. Hoja Geológica 2366-I/2166-III Mina Pirquitas, Provincia de Jujuy (escala 1:250.000). Servicio Geológico Minero Argentino, Instituto de Geología y Recursos Minerales, Boletín 269.

Cole, G.A., 1994. Graptolite-chitinozoan reflectance and its relationship to other geochemical maturity indicators in the Silurian Qusaiba Shale, Saudi Arabia. Energy Fuel 8, 1443–1459.

Coutand, I., Cobbold, P.R., de Urreiztieta, M., Gautier, P., Chauvin, A., Gapais, D., Rosello, E. A., López-Gamundí, O., 2001. Style and history of Andean deformation, Puna plateau, northwestern Argentina. Tectonics 20 (2), 210–234.

Craig, J.R., Segal, S.J., Zappettini, E.O., 1995. El distrito aurífero Rinconada, Provincia de Jujuy, República Argentina. Congreso Latinoamericano de Geología, No. 10, Actas 2, 22–35.

Dalenz-Farjat, A., Alvarez, L.A., Hernández, R.M., Albariño, L.M., 2002. Cuenca Siluro-Devónica del sur de Bolivia y del noroeste argentino: algunas interpretaciones. Congreso de Exploración y Desarrollo de Hidrocarburos, No. 5, 222–248.

Do Campo, M., Nieto, F., Albanesi, G.L., Ortega, G., Monaldi, R., 2017. Outlining the thermal posdepositional evolution of the Ordovician successions of northwestern Argentina by clay mineral analysis, chlorite geothermometry and Kübler index. Andean Geology 44 (2), 179–212.

Ege, H., Sobel, E.R., Scheuber, E., Jacobshagen, V., 2007. Exhumation history of the southern Altiplano plateau (southern Bolivia) constrained by apatite fission track thermochronology. Tectonics 26 (1), 1–24, TC1004.

Egenhoff, S.O., 2007. Life and death of a Cambrian–Ordovician basin: An Andean three-act play featuring Gondwana and the Arequipa-Antofalla terrane. Geological Society of America Special Papers 423, 511–524.

Epstein, A.G., Epstein, J.B., Harris, L.D., 1977. Conodont color alteration–an index to organic metamorphism. Geological Survey Professional Paper 995, 1–27.

Escayola, M.P., van Staal, C.R., Davis, W.J., 2011. The age and tectonic setting of the Puncoviscana Formation in northwestern Argentina: An accretionary complex related to Early Cambrian closure of the Puncoviscana Ocean and accretion of the Arequipa-Antofalla block. Journal of South American Earth Sciences 32 (4), 438–459.

Fernández, R., Guerrero, C., Manca, N., 1982. El límite Cámbro-Ordovícico en el tramo medio y superior de la quebrada de Humahuaca, Provincia de Jujuy, Argentina. 5to Congreso Latinoamericano de Geología, Actas 1, 3–22.

Forsythe, R.D., Davidson, J., Mpodozis, C., Jesinkey, C., 1993. Lower Paleozoic relative motion of the Arequipa Block and Gondwana; Paleomagnetic evidence from Sierra de Almeida of northern Chile. Tectonics 12 (1), 219–236.

Gentzis, T., de Freitas, T., Goodarzi, F., Melchin, M., Lenz, A., 1996. Thermal maturity of Lower Paleozoic sedimentary successions in Arctic Canada. American Association of Petroleum Geologists Bulletin 80, 1065–1084.

Gohrbandt, K.H.A., 1992. Paleozoic paleogeographic and depositional developments on the central proto-Pacific margin of Gondwana: Their importance to hydrocarbon accumulation. Journal of South American Earth Sciences 6 (4), 267–287.

González, M.A., Pereyra, F., Ramallo, E., Tchilinguirian, P., 2003. Hoja Geológica 2366-IV, Ciudad de Libertador General San Martín, provincias de Jujuy y Salta.

Instituto de Geología y Recursos Minerales, Servicio Geológico Minero Argentino, Boletín 274.

Goodarzi, F., 1984. Organic petrography of graptolite fragments from Turkey. Marine and Petroleum Geology 1, 202–210.

Goodarzi, F., 1985. Reflected light microscopy of chitinozoan fragments. Marine and Petroleum Geology 2, 72–78.

Goodarzi, F., Norford, B., 1985. Graptolites as indicators of the temperature histories of rocks. Journal of the Geological Society 142, 1089–1099.

Goodarzi, F., Higgins, A.C., 1987. Optical properties of sclerodonts and their use as indicators of thermal maturity. Marine and Petroleum Geology 14, 353–359.

Goodarzi, F., Norford, B., 1987. Optical properties of graptolite epiderm–a review. Bulletin of the Geological Society of Denmark 35, 141–147.

Goodarzi, F., Norford, B., 1989. Variation of graptolite reflectance with depth of burial. International Journal of Coal Geology 11, 127–141.

Goodarzi, F., Stasiuk, L.D., Lindholm, K., 1988. Graptolite reflectance and thermal maturity of Lower and Middle Ordovician shale from Scania, Sweden. Geologiska Föreningen i Stockholm Förhandlingar 110 (3), 225–236.

Goodarzi, F., Fowler, M.G., Bustin, M., McKirdy, D.M., 1992a. Thermal maturity of Early Paleozoic sediments as determined by the optical properties of marine–derived organic matter–A Review. Early Organic Evolution, 279–295.

Goodarzi, F., Gentzis, T., Harrison, J.C., Thorsteinsson, R., 1992b. The significance of graptolite reflectance in regional thermal maturity studies, Queen Elizabeth Islands, Arctic Canada. Organic Geochemistry 18, 347–357.

Grahn, Y., Gutierrez, P.R., 2001. Silurian and Middle Devonian Chitinozoa from the Zapla and Santa Barbara Ranges, Tarija Basin, northwestern Argentina. Ameghiniana 38, 35–50.

Hao, J., Zhong, N., Luo, Q., Dehan, L., Wu, J., Liu, A., 2019. Raman spectroscopy of graptolite periderm and its potential as an organic maturity indicator for the Lower Paleozoic in southwestern China. International Journal of Coal Geology 213, https://doi.org/10.1016/j.coal.2019.103278

Hartkopf-Fröder, C., Königshof, P., Littke, R., Schwarzbauer, J., 2015. Optical thermal maturity parameters and organic geochemical alteration at low grade diagenesis to anchimetamorphism: a review. International Journal Coal Geology 150–151, 74–119.

Herrera Sánchez, N.C., Toro, B.A., Lo Valvo, G.A., 2019. Lower–Middle Ordovician graptolite biostratigraphy and future challenges for the Central Andean Basin (NW Argentina and S Bolivia), in: Obut, O.T., Sennikov, N.V., Kipriyanova, T.P. (Eds.), Contributions of the 13th International on the Ordovician System. Novosibirsk: Publishing House of SB RAS, pp. 71–74.

Hongn, F.D., Vaccari, N.E., 2008. La discordancia Tremadociano superior-Arenigiano inferior en Vega Pinato (Salta): Evidencia de deformación intraordovícica en el borde occidental de la Puna, in: Coira, B., Zappetteni, E.O. (Eds.), Geología y recursos naturales de la provincia de Jujuy, Relatorio del 17° Congreso Geológico Argentino, Buenos Aires: Asociación Geológica Argentina, pp. 1299–1300.

İnan, S., Goodarzi, F., Mumm, A.S., Arouri, K., Qathami, S., Ardakani, O.H., İnan, T., Tuwailib, A.A., 2016. The Silurian Qusaiba Hot Shales of Saudi Arabia: an integrated assessment of thermal maturity. International Journal of Coal Geology 159, 107–119.

ISO 7404-2., 2009. Methods for the Petrographic Analysis of Coals - Part 2: Methods of Preparing Coal Samples. International Organization for Standardization, 1–12.

ISO 7404-5., 2009. Methods for the Petrographic Analysis of Coals - Part 5: Method of Determining Microscopically the Reflectance of Vitrinite. International Organization for Standardization, 1–14.

Jacobshagen, V., Müller, J., Wemmer, K., Ahrendt, H., Manutsoglu, E., 2002. Hercynian deformation and metamorphism in the Cordillera Oriental of Southern Bolivia, Central Andes. Tectonophysics 345, 119–130.

Kley, J., Reinhardt, M., 1994.Geothermal and tectonic evolution of the Eastern Cordillera and the Subandean Ranges of Southern Bolivia, in: Reutter, K.J., Scheuber, E., Wigger, P.J. (Eds.), Tectonics of the Southern Central Andes. Structure and Evolution of an Active Continental Margin. Springer Verlag, pp. 155–170.

Kurylowicz, L., Ozimic, S., Mckirdy, D., Kantsler, A., Cook, A., 1976. Reservoir and source rock potential of the Larapinta Group, Amadeus Basin, central Australia. Australian Petroleum Exploration Association Journal 16, 49–65.

Lo Valvo, G.A., Herrera Sánchez, N.C., Toro, B.A., 2020. Early-Middle Ordovician graptolites from the Argentine Puna: quantitative paleobiogeographic analysis based on a systematic revision. Ameghiniana 57 (6), 534–554.

Luo, Q., Zhong, N., Dai, N., Zhang, W., 2016. Graptolite-derived organic matter in the Wufeng–Longmaxi Formations (Upper Ordovician–Lower Silurian) of southeastern Chongqing, China: implications for gas shale evaluation. International Journal of Coal Geology 153, 87–98.

Luo, Q., Hao, J., Skovsted, C.B., Luo, P., Khan, I., Wu, J., Zhong, N., 2017. The organic petrology of graptolites and maturity assessment of the Wufeng–

Longmaxi Formations from Chongqing, China: Insights from reflectance cross-plot analysis. International Journal of Coal Geology 183, 161–173.

Luo, Q., Hao, J., Skovsted, C.B., Xu, Y., Liu, Y., Wu, J., Zhang, S., Wang, W., 2018. Optical characteristics of graptolite-bearing sediments and its implication for thermal maturity assessment. International Journal of Coal Geology 195, 386–401.

Luo, Q., Goodarzi, F., Zhong, N., Wang, Y., Qiu, N., Skovsted, C., Suchý, V., Hemmingsen Schovsbo, N., Morga, R., Xu, Y., Hao, J., Liu, J., Wu, J., Cao, W., Min, X., Wu, J., 2020. Graptolites as fossil geo-thermometers and source material of hydrocarbons: an overview of four decades of progress. Earth-Science Reviews 200, https://doi.org/10.1016/j.earscirev.2019.103000

Maletz, J., Lenz, A.C., Bates, D.E., 2016. Part V, Second Revision, Chapter 4: Morphology of the Pterobranch Cubarium. Treatise Online 76, 1–63.

Maletz, J., Toro, B.A., Zhang, Y.D., VandenBerg, A.H.M., 2018a. Part V, Second Revision, Chapter 20: Suborder Dichograptina: Introduction, Morphology, and Systematic Descriptions. Treatise Online 108, 1–28.

Maletz, J., Zhang, Y.D., VandenBerg, A.H.M., 2018b. Part V, Second Revision, Chapter 19: Suborder Sinograptina: Introduction, Morphology, and Systematic Descriptions. Treatise Online 107, 1–23.

Mángano, M.G., Buatois, L.A., 2004. Integración de estratigrafía secuencial, sedimentología e icnología para un análisis cronoestratigráfico del Paleozoico inferior del noroeste argentino. Revista de la Asociación Geológica Argentina 59 (2), 273–280.

Martínez, M., Brussa, E.D., Pérez, B., Coira, B., 1999. El Ordovícico de la Sierra de Quichagua (Puna oriental argentina): litofacies volcanosedimentarias y graptofaunas. Actas de 14° Congreso Geológico Argentino, 347–350.

Marquillas, R.A., Matthews, S.J., 1996. Skarn formation beneath Lascar volcano, N Chile: evidence for the western continuation of the Yacoraite Formation (Late Cretaceous) of NW Argentina. III Symposium International sur la Géodynamique Andine, 431–434.

Marquillas, R.A., del Papa, C., Sabino, I.F., 2005. Sedimentary aspects and paleoenvironmental evolution of a rift basin: Salta Group (Cretaceous–Paleogene), northwestern Argentina. International Journal of South American Earth Sciences 94, 94–113.

Mon, R., Hongn, F.D., 1991. The structure of the Precambrian and Lower Paleozoic basement of the Central Andes between 22° and 32° S. Lat. Geologische Rundschau 80, 745–758.

Mon, R., Salfity, J.A., 1995. Tectonic evolution of the Andes of Northern Argentina, in: Tankard, A.J., Suárez, R., Welsink, H.J. (Eds.), Petroleum Basins of South America. American Association of Petroleum Geology, Memoir 62, pp. 269–283.

Mon, R., Hongn, F., 1996. Estructura del basamento proterozoico y paleozoico inferior del norte argentino. Revista de la Asociación Geológica Argentina 51 (1), 3–14.

Monteros, J.A., Moya, M.C., Monaldi, C.R., 1996. Graptofaunas arenigianas el borde occidental de la Puna Argentina. Implicancias paleogeográficas. Memorias del 12° Congreso Geológico de Bolivia 2, 733–746.

Moretti, I., Baby, P., Mendez, E., Zubieta, D., 1996. Hydrocarbon generation in relation to thrusting in the Sub Andean zone from 18 to 22°S, Bolivia. Petroleum Geoscience 2 (1), 17–28.

Moya, M.C., 1998. Lower Ordovician in the southern part of the argentine eastern cordillera, in: Bahlburg, H., Breitkreuz, C., Giese, P. (Eds.), The Southern Central Andes: Contributions to Structure and Evolution of an Active Continental Margin. Springer Berlin Heidelberg, Berlin, Heidelberg, pp. 55–69.

Moya, M.C., 1999. El Ordovícico en los Andes del norte argentino, in: González Bonorino, G., Omarini, R., Viramonte, J. (Eds.), Geología del Noroeste Argentino. Congreso Geológico Argentino, No. 14, Relatorio I, Buenos Aires: Asociación Geológica Argentina, pp. 134–152.

Moya, M.C., 2003. The Ordovician System in the Argentina Eastern Cordillera, in: Ordovician and Silurian of the Cordillera Oriental and Sierras Subandinas, NW Argentina. Field Trip Guide. Instituto Superior de Correlación Geológica (INSUGEO), Serie Correlación Geológica 11, pp. 7–16.

Moya, M.C., 2015. La "Fase Oclóyica" (Ordovícico Superior) en el noroeste argentino. Interpretación histórica y evidencias en contrario. Instituto Superior de Correlación Geológica (INSUGEO), Serie Correlación Geológica 31 (1), 73–110.

Moya, M.C., Monteros, J.C., 1999. El Ordovícico tardío y el Silúrico en el borde Occidental de la Cordillera Oriental Argentina. 14º Congreso Geológico Argentino, Actas 1. Buenos Aires: Asociación Geológica Argentina, 401–404.

Obermayer, M., Fowler, M.G., Goodarzi, F., Snowdon, L.R., 1996. Assessing thermal maturity of Palaeozoic rocks from reflectance of chitinozoa as constrained by geochemical indicators: an example from southern Ontario, Canada. Marine and Petroleum Geology 13, 907–919.

Petersen, H.I., Schovsbo, N.H., Nielsen, A.T., 2013. Reflectance measurements of zooclasts and solid bitumen in Lower Palaeozoic shales, southern Scandinavia:

correlation to vitrinite reflectance. International Journal of Coal Geology 114, 1–18.

Ramos, V., Jordan T., Allmendinger R., Kay S., Cortés J., Palma M., 1984. Chilenia: un terreno alóctono en la evolución paleozoica de los Andes centrales. IX Congreso Geológico Argentino, Buenos Aires: Asociación Geológica Argentina 2, 84–106.

Rubiolo, D., Seggiaro, R., Gallardo, E., Disalvo, A., Sánchez, M., Turel, A., Ramallo, E., Sandruss, A., Godeas, M., 2003. Hoja Geológica 2366-II / 2166-IV, La Quiaca. Provincias de Jujuy y Salta. Servicio Geológico Minero Argentino, Instituto de Geología y Recursos Minerales, Boletín 246.

Ruiz Huidobro, O.J., 1975. El Paleozoico Inferior del centro y sur de Salta y su correlación con el Grupo Mesón. 1er Congreso Argentino de Paleontología y Bioestratigrafía, Actas 1, 91–107.

Salfity, J.A., Marquillas, R.A., 1994. Tectonic and sedimentary evolution of the Cretaceous-Eocene Salta Group Basin, Argentina, in: Salfity, J.A. (Ed.), Cretaceous Tectonics of the Andes. Earth Evolution Sciences, Friedr. Vieweg & Sohn, pp. 266–315.

Sempere, T., 1995. Phanerozoic evolution of Bolivia and adjacent regions, in: Tankard, A.J., Suárez Soruco R., Welsink H.J. (Eds.), Petroleum basins of South America. AAPG Memoir 62, pp. 207–230.

Suárez-Ruiz, I., Flores, D., Mendonça Filho, J.G., Hackley, P.C., 2012. Review and update of the applications of organic petrology: Part 1, geological applications. International Journal of Coal Geology 99, 54–112.

Suchý, V., Sýkorová, I., Stejskal, M., Sâfanda, J., Machovič, V., Novotná, M., 2002. Dispersed organic matter from Silurian shales of the Barrandian Basin, Czech

Republic: optical properties, chemical composition and thermal maturity. International Journal of Coal Geology 53, 1–25.

Starck, D., 1995. Silurian-Jurassic stratigraphy and basin evolution of northwestern Argentina, in: Tankard, A.J., Suárez Soruco R., Welsink H.J. (Eds.), Petroleum basins of South America. AAPG Memoir 62, 251–267.

Starck, D., 2011. Cuenca Cretácica-Paleógena del Noroeste argentino. VIII Congreso de Exploración y Desarrollo de Hidrocarburos Simposio. Cuencas Argentinas: visión actual, Actas, 407–453.

Starck, D., Gallardo, E., Schultz, A., 1992. La discordancia precarbónica en la porción argentina de la Cuenca de Tarija. Boletín de Informaciones Petroleras, Buenos Aires, Argentina, Tercera Época 29, 2–11.

Starck, D., Gallardo, E., Schultz, A., 1993. The pre-Carboniferous unconformity in the Argentine portion of the Tarija Basin. XII International Congress on Carboniferous–Permian 2, 373–384.

Starck, D., Rodriguez, A., Constantini, L., 2002. Los Reservorios de las formaciones Tupambí, Tarija, Las Peñas y San Telmo, in: Schiuma, M., Vergani, G., Hinterwimmer, G. (Eds.): Las rocas reservorio de las cuencas productivas de la Argentina. V Congreso de Exploración y Desarrollo de Hidrocarburos, pp. 699–716.

Tawackoli, S., Kley, J., Jacobshagen, V., 1996. Evolución tectónica de la Cordillera Oriental del sur de Bolivia. Memorias del 12° Congreso Geológico de Bolivia 1, 91–96.

Teichmüller, M., 1978. Nachweis von graptolithen-periderm in geschieferten gesteinen mit hilfe kohlenpetrologischer methoden. Neues Jahrbuch für Geologie und Paläontologie, Monatshefte 7, 430–447.

Toro, B.A., 1993. Graptofauna arenigiana de la Quebrada del río Cajas (Formación Acoite), Provincia de Jujuy, Argentina. Ameghiniana 30 (1), 69–76.

Toro, B.A., 1994. Las zonas de *Didymograptus* (*Didymograptellus*) *bifidus* (Arenigiano medio) y *Didymograptus* (*Corymbograptus*) *deflexus* (Arenigiano inferior) en la Formación Acoite, Cordillera Oriental, Argentina. Ameghiniana 31 (3), 209–220.

Toro, B.A., 1995. Primer hallazgo de graptolitos del Silúrico (Llandoveriano) en la Cordillera Oriental, Provincia de Jujuy, Argentina. Ameghiniana 32, 375–384.

Toro, B.A., 1997. La fauna de graptolitos de la Formación Acoite, en el borde occidental de la Cordillera Oriental Argentina, Análisis bioestratigráfico. Ameghiniana 34 (4), 393–412.

Toro, B.A., Brussa, E.D., 2003. Graptolites, in: Benedetto, J.L. (Ed.), Ordovician fossils of Argentina. Secretaría de Ciencia y Tecnología, Universidad Nacional de Córdoba. pp. 441–505.

Toro, B.A., Maletz, J., 2007. Deflexed *Baltograptus* species in the early to mid Arenig Graptolite Biostratigraphy of northwestern Argentina. Acta Palaeontologica Sinica 46, 489–496.

Toro, B.A., Maletz, J., 2008. The proximal development in *Cymatograptus* (Graptoloidea) from Argentina and its relevance for the early evolution of the Dichograptacea. Journal of Paleontology 82 (5), 974–983.

Toro, B.A., Vento, B.A., 2013. Reevaluación de las Biozonas de *Tetragraptus phyllograptoides* y *T. akzharensis* (Ordovícico Inferior-Floiano) de la Cordillera Oriental Argentina. Ameghiniana 50, 287–297.

Toro, B.A., Meroi Arcerito, F.R., Muñoz, D.F., Waisfeld, B.G., de la Puente, G.S., 2015. Graptolite-trilobite biostratigraphy in the Santa Victoria area, northwestern

Argentina. A key for regional and worldwide correlation of the Lower Ordovician (Tremadocian - Floian). Ameghiniana 52 (5), 535–557.

Toro, B.A., Herrera Sánchez, N.C., 2019. Stratigraphical distribution of the Ordovician graptolite *Azygograptus* Nicholson & Lapworth in the Central Andean Basin (NW Argentina and S Bolivia). Comptes Rendus Palevol 18 (5), 493–507.

Toro, B.A., Heredia, S., Herrera Sánchez, N.C., Moreno, F., 2020. First Middle Ordovician conodont record related to key graptolites from the western Puna, Argentina: Perspectives for an integrated biostratigraphy and correlation of the Central Andean Basin. Andean Geology 47 (1), 144–161.

Turner, J.C.M., 1960. Estratigrafía de la Sierra de Santa Victoria y adyacencias. Boletín de la Academia Nacional de Ciencias 41, 163–196.

Turner, J.C.M., 1964. Descripción Geológica de la Hoja 2c. Santa Victoria, 99.

Turner, J.C.M., Méndez, V., 1975. Geología del sector oriental de los departamentos de Santa Victoria e Iruya, Provincia de Salta, República Argentina. Boletín de la Academia Nacional de Ciencias de Córdoba 51 (1–2), 11–24.

Turner, J.C.M., Mon, R., 1979. Cordillera Oriental, in: Turner, J.C.M (Ed.), Geología Regional Argentina. Academia Nacional de Ciencias, Publicación Especial 1, pp. 57–94.

Vaucher, R., Vaccari, N.E., Balseiro, D., Muñoz, D.F., Dillinger, A., Waisfeld, B.G., Buatois, L.A., 2020. Tectonic controls on late Cambrian-Early Ordovician deposition in Cordillera Oriental (Northwest Argentina). International Journal of Earth Sciences 109, 1897–1920.

Voldman, G.G., Albanesi, G.L., Ortega, G.C., Giuliano, M.E., Monaldi, C.R., 2017. New conodont taxa and biozones from the Lower Ordovician of the Cordillera Oriental, NW Argentina. Geological Journal 52, 394–414.

Waisfeld, B.G., Astini, R.A., 2003. Environmental constraints on faunal patterns. An example in early Ordovician (Arenig) trilobite assemblages from the Argentine Cordillera Oriental, in: Albanesi G.L., Beresi, M., Peralta S.H. (Eds.), Ordovician from the Andes. Serie Correlación Geológica 17, pp. 341–346.

Waisfeld, B.G., Sánchez, T.M. Benedetto, J.L., Carrera, M.G., 2003. Early Ordovician (Arenig) faunal assemblages from western Argentina. Biodiversification trends in different geodynamic and palaeogeographic settings. Palaeogeography, Palaeoclimatology, Palaeoecology 196, 343–373.

Weishauptová, Z., Přibyl, O., Sýkorová, I., René, M., 2017. Effect of the properties of Silurian shales from the Barrandian Basin on their methane sorption potential. Fuel 203, 68–81.

Zimmermann, U., 2011. From fore-arc to foreland: a cross section of the Ordovician in the Central Andes, in: Gutiérrez Marco, J.C., Rábano, I., García-Bellido, D. (Eds.), Ordovician of the World. Cuadernos del Museo Geominero 14, pp. 667–674.

Zimmermann, U., Bahlburg, H., 2003. Provenance analysis and tectonic setting of the Ordovician clastic deposits in the southern Puna basin, NW Argentina. Sedimentology 50, 1079–1104.

FIGURE CAPTIONS

Figure 1. a) Location map of the geomorphological provinces comprised in the Central Andean Basin. **b)** Geological map of the studied area showing sampling localities with conodont and graptolite biostratigraphic control (Modified from González *et al.*, 2003).

Figure 2. Stratigraphic section from the Los Colorados area, Cordillera Oriental (Modified from Astini *et al.*, 2004) showing the position of the samples. **GB:** Graptolite biozone.

Figure 3. Stratigraphic sections from the Argentine Puna showing the position of the samples. **a)** Huaytiquina area, western Puna (Modified from Monteros *et al.*, 1996). **b)** Muñayoc area, eastern Puna (Modified from Martínez *et al.*, 1999). **GB:** Graptolite biozone.

Figure 4. Summary table with the provenance and taxonomy of the graptolite samples.

Figure 5. Photomicrographs of polished fragments of graptolite from the Puna region (Muñayoc section) under reflected plane-polarized light. **(a)** MU-12; **(b)** MU-12; **(c)** MU 9+1 m; **(d)** MU-11; **(e)** MU-11; **(f)** M//U-15. The scale bar is 10 micrometers.

Figure 6. Photomicrographs of polished fragments of graptolite from the Puna region (Muñayoc section) under reflected plane-polarized light. **(a)** MU-11; **(b)** MU-11; **(c)** MU 9+1 m; **(d)** MU-6; **(e)** MU-15; **(f)** MU-15. The scale bar is 10 micrometers.

Figure 7. Photomicrographs of polished fragments of graptolite from the Puna (Huaytiquina section) and Cordillera Oriental (Los Colorados section) regions under reflected plane-polarized light. **(a)** RH-A; **(b)** LC-17; **(c)** LC-17; **(d)** LC-24+40m; **(e)** LC-14; **(f)** LC-17. The scale bar is 10 micrometers.

Figure 8. Histograms of the %GRo measurements of the six samples from the Los Colorados section. **(a)** Sample LC-12; **(b)** Sample LC-14; **(c)** Sample LC-17; **(d)** Sample LC-21; **(e)** Sample LC-24+40m; **(f)** Sample LC-FL.

Figure 9. Thermal maturity modeling of vitrinite reflectance for the Los Colorados section, Cordillera Oriental Argentina using PetroMod 1D Express software. Red stars represent the middle part of the Acoite Formation where the LC-17, LC-21, and LC-24+40m graptolite samples come from.

THERMAL HISTORY OF THE NORTHWESTERN ARGENTINA, CENTRAL ANDEAN BASIN, BASED ON FIRST-EVER REPORTED GRAPTOLITE REFLECTANCE DATA

Nexxys C. Herrera Sánchez[1], Blanca A. Toro[1], Ricardo Ruiz-Monroy[2], Thomas Gentzis[3], Seare Ocubalidet[3] and Humberto Carvajal-Ortiz[3]

[1]Centro de Investigaciones en Ciencias de la Tierra (CICTERRA), Universidad Nacional de Córdoba, Facultad de Ciencias Exactas, Físicas y Naturales, Consejo Nacional de Investigaciones Científicas y Tecnológicas (CONICET), Av. Vélez Sarsfield 1611, X5016CGA, Córdoba, Argentina. nexxys.herrera@unc.edu.ar; btorogr@mendoza-conicet.gob.ar

[2]Helmholtz Centre Potsdam-GFZ. German Research Centre for Geosciences, Section 3.2: Organic Geochemistry, Wissenschaftpark "Albert Einstein", Telegrafenberg, 14473, Potsdam, Germany. ricardoruizmonroy@yahoo.com

[3]Core Laboratories, 6316 Windfern Road, TX 77040, Houston, Texas, United States. thomas.gentzis@corelab.com; seare.ocubalidet@corelab.com; humberto.carvajal@corelab.com

42 pages; 9 figures; 2 tables

Corresponding author: Nexxys C. Herrera Sánchez, nexxys.herrera@unc.edu.ar

ABSTRACT. The thermal maturity from the early Paleozoic strata in Northwestern Argentina was studied using reflected light microscopy and Rock-Eval analyses. The graptolites were collected from the Acoite and Lipeón formations, from the Los Colorados section, Cordillera Oriental, and the Huaytiquina, and Muñayoc sections, Puna highland, corresponding to the "Coquena" Formation and the Cochinoca-Escaya Magmatic-Sedimentary Complex. Rock-Eval parameters were unreliable due to the low TOC, S1, and S2 values. The Cordillera Oriental region sediments have low maturity based on low reflectance (%GRo= 0.63%-1.11%) and anisotropy of graptolite. In contrast, the higher graptolite reflectance of samples from the Muñayoc and Huaytiquina sections (%GRo= 5.57%-6.62%), in the Puna region, indicates considerably higher maturity. This could result from the combination of hydrothermal fluids with a temperature range from 336 °C to 358 °C, associated volcanism, and deformation related to tectonics events which produced a higher geothermal gradient in the Puna. The Los Colorados section's thermal maturity modeling shows a better fit considering erosion episodes at the Late Paleozoic and Early Cenozoic. However, more studies about geothermal parameters and stratigraphy are necessary to corroborate these preliminary models and propose new approaches for the Puna region.

Keywords: Graptolites, Thermal Maturity, Northwestern Argentina, Ordovician, Equivalent Vitrinite Reflectance.

6. INTRODUCTION

The reflectance of bitumen, zooclasts, and vitrinite-like particles has been widely used to evaluate the thermal maturity in pre-Devonian rocks, in which primary vitrinite is absent (Kurylowicz *et al*., 1976; Goodarzi, 1984, 1985; Goodarzi and Norford, 1985, 1989; Goodarzi and Higgins, 1987; Goodarzi *et al.*, 1988; Obermayer *et al.*, 1996; Suchý *et al*., 2002; Petersen *et al*., 2013; İnan *et al.*, 2016; Luo *et al*., 2016, 2017, 2018; between others). Graptolites, conodonts, chitinozoans, and scolecodonts are commonly preserved in Early Palaeozoic rocks, and their optical properties have been widely studied (Suárez-Ruiz *et al.*, 2012; Petersen *et al*., 2013; Hartkopf-Fröder *et al.*, 2015 and references therein). Among these zooclasts, graptolites are probably the most widely used group for thermal maturity studies because of their greater abundance and wide distribution in most sedimentary lithofacies and paleoenvironments (Cole, 1994; Petersen *et al*., 2013).

Modern studies about the tubarium, the housing of planktic graptolites, confirm that it is a complexly organized organic structure produced in distinct increments called the *fuselli*. The material of the fossil graptolite tubarium consists of an aliphatic polymer and does not contain any protein, even though the structure and analysis of the housing material of modern pterobranchs indicate that it was originally collagen (Maletz *et al.*, 2016). The tubarium structure is composed of individual zooidal tubes termed the *thecae* that are interconnected through a common canal from the *sicula*, a differentiated housing from the colony founder. The two basic constructional features of the thecae are the fusellum (fusellar layer) and the *cortex* (cortical layer). Each fusellus possesses at least one oblique suture and is stacked one upon another with some lateral overlap to form a distally open tube. The cortex is secreted in distinct bandages on the surface of the thecal tubes (Maletz *et al.*, 2016: figs. 1, 4).

Graptolites were used for the first time as thermal indicators by Kurylowicz *et al*. (1976). They noted that the reflectance and optical properties of graptolite fragments in Ordovician strata of the Amadeus Basin, Australia, closely resemble those of the vitrinite. Since then, graptolites in different Ordovician, and Silurian basins, from Australia, Saudi Arabia, China, Germany, Sweden, Turkey, Canada, Poland, USA, Austria, and the Czech Republic, have been widely used for thermal maturation studies in a wide range of geological applications (metamorphic subfacies, hydrocarbon, and mineral exploration, and contact metamorphism) (Goodarzi *et al*., 1992a-b; Gentzis *et al*., 1996; Suárez-Ruiz *et al*., 2012; Hartkopf-Fröder *et al*., 2015; Weishauptová *et al*., 2017; Luo *et al*., 2016, 2017, 2018, 2020, and references therein).

The relationship between graptolite reflectance, and other thermal parameters such as equivalent vitrinite reflectance (VRo-eq), equivalent solid bitumen reflectance (BRo-eq), Rock-Eval pyrolysis Tmax, Thermal Alteration Index (TAI), and Conodont Color Alteration Index (CAI) has been established throughout the years. Goodarzi and Norford (1989) indirectly correlated the graptolite maximum reflectance with vitrinite reflectance using the CAI and described that vitrinite has a lower reflectance value than graptolite for the same CAI. Later, Petersen *et al*. (2013) determined a relationship between the random reflectance of graptolites and vitrinites through the intermediate conversion of Rock-Eval pyrolysis Tmax values, and illustrated that the graptolite random reflectance (GRo, ran) is higher than vitrinite random reflectance (VRo, ran). These authors also indicated that the maximum reflectance (Ro, max) increases gradually with burial depth. Hence, the reflectance can be used to study the burial history and maturity of Paleozoic successions. Hartkopf-Fröder *et al.* (2015) summarized the stages of oil and gas generation, and the correlation between vitrinite reflectance in coal, and optical and thermal maturity parameters including CAI,

Transmittance Color Index (TCI), Acritarch Colour Alteration Index (AAI), Spore Colour Index (SCI), Graptolite Reflectance, and Thermal Alteration Index (TAI).

Furthermore, Luo *et al.* (2018) showed that graptolite random reflectance is a better thermal maturity indicator than graptolite maximum reflectance and is more precise due to its smaller standard deviation. These authors also proposed equations to determine the thermal maturity of the graptolite-bearing sediments based on graptolite random reflectance, graptolite maximum reflectance, and solid bitumen random reflectance. Recently, Hao *et al.* (2019) used the relationship between vitrinite reflectance and graptolite reflectance proposed by Luo *et al.* (2018), and suggested a conversion equation of the equivalent vitrinite reflectance, based on Raman spectroscopy values of the graptolite tubarium structure, to assess the thermal maturity of the Early Paleozoic sequence in southwestern China. Luo *et al.* (2020) reviewed previous studies on graptolite reflectance, and presented a new equation to correlate random graptolite reflectance to equivalent vitrinite reflectance.

Studies concerning the thermal maturity of Ordovician rocks remain scarce for the Early Paleozoic sequences in the Central Andean Basin. Kley and Reinhardt (1994) used reflectance and infrared spectroscopy measurements of the organic matter to determine the organic matter maturity in Southern Bolivia. They concluded that maturity varies from very weakly diagenetic in the Subandean Ranges to low-grade metamorphic in the Eastern Cordillera.

Previous research related to geothermal studies in Northwestern Argentina was based mainly on CAI. Carlorosi *et al*. (2013) determined a 1.5- 2 CAI (*sensu* Epstein *et al*., 1977) in conodonts from the *Baltoniodus triangularis* Zone (Dp1, *sensu* Bergström *et al.*, 2009) in the Los Colorados area, Cordillera Oriental. Later, Voldman *et al*. (2017) assigned a CAI value of 3 to some specimens from the *Acodus triangularis*, *Gothodus*

vetus, and *Gothodus andinus* biozones (Tr3-Fl2). The above CAI value accounts for burial paleotemperatures ranging from 110-200 °C (*sensu* Epstein *et al*., 1977) in the Chulpios Creek, Santa Victoria area, Cordillera Oriental. Afterward, Toro *et al*. (2020) recognized conodonts of the *Baltoniodus navis* Zone with a CAI of 1.5-2 of the Epstein *et al.* (1977) scale in the Huaytiquina area Western Puna. Based on CAI and analysis of clay minerals, Do Campo *et al.* (2017) calculated the paleotemperatures for metapelites and metavolcanic rocks of the Late Cambrian-Ordovician succession in Northwestern Argentina. They concluded that there is an E-W trend ranging from diagenesis/low anchizone in the eastern flank of the Santa Victoria Range, to high anchizone/epizone in the Puna region, with intermediate values in the western flank of the Santa Victoria Range.

Graptolites from Northwestern Argentina have been studied for more than a century allowing for regional and intercontinental biostratigraphic correlations to be established (Turner, 1960; Toro 1995, 1997; Brussa *et al.*, 2008; Toro and Vento, 2013; Toro *et al*., 2015; Albanesi and Ortega, 2016; Toro and Herrera Sánchez, 2019; Herrera Sánchez *et al*., 2019) but have not been used as thermal maturity indicators up to now.

This study provides, for the first time, an early interpretation and discussion about the thermal postdepositional evolution for the Central Andean Basin in Northwestern Argentina (Fig. 1) based on graptolite reflectance, and Rock-Eval pyrolysis data.

Figure 1. Location map (size: 2-column)

7. GEOLOGICAL FRAMEWORK

The Central Andean Basin (Sempere, 1995) developed in an active margin of the western Gondwana during the Cambrian-Ordovician. It spreads over Northwestern

Argentina (NWA) and encompasses parts of Chile, Bolivia, and Perú (Astini, 2003). NWA includes, from West to East, the geomorphological provinces of Puna, Cordillera Oriental, Sierras Subandinas, and Sierras de Santa Bárbara (Fig. 1a). This study focuses on the Ordovician strata outcrops in the Puna region and the Ordovician and Early Silurian deposits exposed in the Cordillera Oriental.

The basement of the studied area is represented by the Vendian-Early Cambrian Puncoviscana Formation (Turner, 1960), which is composed mainly of a pelite-greywacke turbidite sequence. It has been affected by very low-grade metamorphism and polyphase deformation during the Early Cambrian Pampean Orogeny (Mon and Hongn, 1996; Escayola *et al*., 2011, Casquet *et al*., 2018). This unit is unconformably overlain by Middle-Late Cambrian shallow platform quartzites, sandstones, and red to greenish shales of the Mesón Group. In turn, the above group is unconformably overlain by the Late Cambrian-Early Ordovician rock succession. This unconformity is related to the rifting phase ("Irúyica Phase"; Turner and Méndez, 1975), and the eastern movement of the Arequipa-Antofalla terrain (AAt) that resulted in the opening of a V-shaped marine basin that widened northward towards Bolivia (Gohrbandt, 1992; Forsythe *et al*., 1993; Bahlburg and Hervé, 1997; Egenhoff, 2007). Alternatively, this contact has been considered as an unconformity resulting from a relative sea-level fall (Moya, 1998; Buatois *et al*., 2000; Buatois and Mángano, 2003; Mángano and Buatois, 2004) or even being a conformable depositional transition (Ruiz Huidobro, 1975; Fernández *et al*., 1982). Recently, Vaucher *et al.* (2020) recognized an episode of basin deformation around the Cambrian-Ordovician transition in NWA. These authors associated this stratigraphic unconformity to the onset of the retro-arc basin in the Cordillera Oriental, which probably occurred earlier in the western/southwestern foredeep area near the volcanic arc developed in the Puna region.

The Late Cambrian-Ordovician sedimentary sequence from the Cordillera Oriental corresponds to the Santa Victoria Group (Turner, 1964), which includes the Santa Rosita (Late Cambrian-Tremadocian), and the Acoite (Floian-Early Dapingian) formations (Astini, 2003; Buatois and Mángano, 2003; Toro *et al.*, 2015; Toro and Herrera Sánchez, 2019). In the Puna region, the fossiliferous siliciclastic marine sediments assigned to the Late Cambrian, Tremadocian, and Floian interfingering with synsedimentary lavas, and subvolcanic intrusives that were grouped into three complexes based on distinctive facies, namely the Puna Volcanic Complex, the Puna Turbidite Complex, and the Puna Shelf Complex (Zimmermann and Bahlburg, 2003; Zimmermann, 2011). On the other hand, Coira *et al.* (2004) defined the Cochinoca-Escaya Magmatic-Sedimentary Complex (CEMSC) as being composed of volcaniclastic dacites intercalated with medium- to fine-grained sandstones and massive pelites. CEMSC outcrops in the Cochinoca-Escaya, Queta, and Quichagua Ranges, eastern Puna. It is associated with volcanic breaches, hyaloclastites, cryptodomes, massive spilitized basaltic levels or padded structures, and micro-gabbros forming layers or lacolites (Coira, 2008, and references therein). The best outcrops of this complex are found in the Muñayoc section located in the Quichagua Range, Jujuy Province (Fig. 1b).

The Ordovician succession in NWA was folded by a simple structural style and was intruded by granite (Mon and Hongn, 1991). The intensity of folding increases gradually westward, from less deformed sequences such as those of the Cordillera Oriental to beds affected by intense west-verging folding with east-dipping axial plane cleavage in the Puna region (Mon and Hongn, 1991). The outcrops of Ordovician beds depicting tight folds covered unconformably by Silurian and Devonian beds were included by Mon and Hongn (1991) in the "Ocloyic Belt", with the age of deformation attributed traditionally to the "Ocloyic Phase" (Late Ordovician) (Turner and Méndez,

1975; Turner and Mon, 1979; Mon and Hong, 1991; Mon and Salfity, 1995, between others). This intra-Ordovician deformation has been documented in several outcrops of Early Ordovician rocks in the transition between Puna and the Cordillera Oriental as well as in the Salar del Rincón area, western Puna (Bahlburg, 1990; Bahlburg and Hervé, 1997; Moya, 1999; Astini, 2003; Hongn and Vaccari, 2008). On the other hand, Moya (1999, 2003, 2015) discussed the conceptual framework in which the "Ocloyic Phase" was defined. This author proposed that the Paleozoic deposits were only subject to block tectonics and later folded together with Cretaceous deposits as a result of the Andean Orogeny. The lack of evidence of an angular unconformity separating the Late Ordovician deposits outcropping in the Argentine Cordillera Oriental from the overlying Early Paleozoic sequences supports the interpretation of this author. Besides, K-Ar ages of fine-grained micas obtained for Ordovician very low-grade metapelites of the Bolivian Cordillera Oriental do not show the existence of an orogenic activity during the Late Ordovician. Therefore, the deformation was attributed to either a Late Devonian-Early Carboniferous event (Kley and Reinhardt, 1994; Tawackoli *et al*., 1996) or to a Late Carboniferous-Early Permian orogenic episode (Jacobshagen *et al*., 2002). Astini (2002) considered that the "Ocloyic Phase" comprises a combination of eustatic decay due to the rapid growth phase of the Gondwanic ice sheet and subordinate tectonics.

During the Silurian-Devonian times, the different southwestern Gondwana basins were generally grouped as underfilled shallow marine basins (Starck, 1995 and references therein). At NWA, and southern Bolivia, approximately 3000 m of siliciclastic rocks were deposited between the Ludlowian-Frasnian (57 My) (Dalenz-Farjat *et al.*, 2002). At the beginning of the Carboniferous, another diastrophic event occurred in NWA. It was probably related to a minor reorganization of the Chilenian

Terrain edge relative to Gondwana, referred to as the "Chanic Phase" (Starck, 1995). Ramos *et al.* (1984) interpreted this phase as a collisional event in plate tectonics terms. Although this orogeny was not intense in the study area, the diastrophism, and hiatus represent the onset of a new tectonostratigraphic cycle, and formation of the Tarija Basin, in the south of Bolivia, and Sierras Subandinas belt at NWA, which is considered as an intracratonic basin with a low subsidence rate (Starck *et al.*, 2002). It is probable that a large part of the Cordillera Oriental remained emerged at this time, which would explain the scarce Siluro-Devonian deposits and also the erosional truncation of the Santa Victoria Group (Starck, 1995). The Carboniferous deposits from NWA are separated from the Devonian succession by a major unconformity related to the "Chanic Phase" (Starck *et al.* 1992, 1993 and references therein), resulting in a hiatus of approximately 50 My (Starck, 1995).

In the Tarija Basin, the Carboniferous-Jurassic interval is characterized by various depositional sequences. The base of the succession overlies a major regional unconformity that is locally modified by deep erosion. This unconformity is most pronounced in the southwestern part of the area where the Silurian-Devonian section in parts of the Cordillera Oriental is completely eroded (Starck, 1995: fig. 6). A network of deeply eroded paleovalleys is deposited on this regional unconformity, incising different levels of the Devonian rocks (Starck *et al.*, 1992, 1993). In the Early Jurassic, a new event resulted in a widespread unconformity and marked a change in regional stress fields. In NWA, an important change in the style of subsidence occurred with the Late Jurassic "Araucanian Phase", which effectively concluded with the development of the Tarija Basin. The extension dissected the old epeiric basin into a suite of fault-controlled half-grabens. Here, the Cretaceous-Paleogene Salta Group developed as a rift basin fill (Starck, 1995, 2011 and references therein).

2.1 Argentine Cordillera Oriental

The Cordillera Oriental is a high relief "thick-skinned type" thrust system with dominant east vergence, in which the Acoite Formation consists of thick, upward-shallowing beds related to a storm-dominated deltaic system (Astini, 2003; Waisfeld and Astini, 2003). The Los Colorados area is located approximately 23˚ 33' S, and 65˚ 40' W in the Jujuy Province (Fig. 1b). The stratigraphy appears to be complete, but most of the described units are separated by stratigraphic discontinuities, such as relative fall surfaces, subaerial exposure, transgressive episodes, or coplanar surfaces. However, these surfaces do not always have an obvious expression from a stratigraphic perspective (Astini *et al.*, 2004). In this area, the Acoite Formation reaches a maximum thickness of almost 2300 m (Waisfeld *et al.*, 2003; Astini *et al.*, 2004; Toro and Herrera Sánchez, 2019) (Fig. 2). It is composed mainly of greenish-gray shale and fine-sandstone, alternating with dark-gray, and black shale, and siltstone deposited in a middle to distal shelf setting (Waisfeld *et al.*, 2003) during the Early Ordovician (*Tetragraptus phyllograptoides*, *T. akzharensis*, *Baltograptus* cf. *B. deflexus*, and *Didymograptellus bifidus* biozones). The upper part of the unit, in which the *Azygograptus lapworthi* Biozone (Middle Ordovician) has been recently recognized in the western side of the Cordillera Oriental by Toro and Herrera Sánchez (2019), is a massive, highly bioturbated sandy facies that developed abruptly, overlying an upward-thickening mesoscale cycle with tidal influence (Astini, 2003; Waisfeld and Astini, 2003). Few meters above these levels, a short interval composed of purplish shales with heterolytic intervals and pale red sandstone with abundant cross-bedded strata (Astini, 2003) is assigned to the Alto del Cóndor Formation (43 m thick) (Astini *et al.*, 2004) (Fig. 2). Carlorosi *et al.* (2013) assigned a short transgressive interval that produces conodonts from the *Baltoniodus triangularis* Zone (Early Dapingian, Dp1) to the Lower

Member of this unit. The overlain Sepulturas Formation (63.5 m thick) (Fig. 2) has a largely coarsening upward arrangement with a variety of open-marine fauna (Astini, 2003). Above it, a regionally extended pebbly-sandy mudstone (Moya and Monteros, 1999) truncates the earlier stratigraphy. This diamictite is known as the Zapla Formation (20 m thick) (Fig. 2) and is relatively well accepted to be of glacial origin, constrained to the uppermost Ordovician, and hence, correlated with the Late Ordovician ice age (Astini, 1999, 2002). The Ordovician succession appears to be in paraconformity with the overlain Silurian deposits (Astini *et al.*, 2004). In the Cordillera Oriental, Early Silurian graptolites (*Stimulograptus sedgwickii*, *Clinoclimacograptus retroversus*, and *Paraclimacograptus innotatus*) were recovered from the overlying strata corresponding to the Lipeón Formation (100 m thick) (Fig. 2) (Toro, 1995), which seem to record an open-shelf environment formed by postglacial transgression (Astini, 2003). Above this unit, the Silurian-Early Devonian deposits of the Arroyo Colorado Formation (Grahn and Gutiérrez, 2001; Aparicio González *et al.*, 2020), reaching 27.5 m in thickness, are constituted by purple-gray muddy, and mottled massive sandstone with good banding development that reflects variable intensities of bioturbation rates (Astini *et al.*, 2004) (Fig. 2). The Paleozoic sequence underlies, by an angular unconformity, the Cretaceous deposits of the Pirgua Subgroup (base of the Salta Group), which represents, in general, ~700 m of a continental sedimentation cycle of red-purple clastic facies. The Pirgua Sg. starts with fluvial facies interdigitating with alluvial-eolian facies in the Tres Cruces subbasin (Fig. 1b) (Boll and Hernández, 1986; Marquillas *et al.*, 2005). It represents the entire *syn-rift* state of the basin infilling, intimately related to direct faults, restricted to distensive grabens, and hemigrabens (Starck, 2011). The *pre-rift* successions were eroded from the rift margins as a result of rift flank uplift. The *post-rift* records two subgroups: the Balbuena Sg., and the Santa Bárbara Sg. The Yacoraite Formation

(Cretaceous-Paleogene; *sensu* Marquillas *et al.*, 2005) included in the Balbuena Sg., mainly consists of 315 m thick of carbonatic rocks exposed in the Espinazo del Diablo (Tres Cruces Basin) which is related to the second Cretaceous marine ingression (Astini *et al.*, 2019).

Figure 2. Stratigraphic column from the Los Colorados area (size: 1.5-column)

2.2 Argentine Puna

The Puna morpho-structural province is a plateau with average highs above 3500 m. The Early Paleozoic is represented by sedimentary deposits and associated volcanism. It is widely accepted that the region comprises two submeridional belts, corresponding to the western and eastern, which were developed from a Cambrian rift margin to a Floian back-arc until a Darriwilian turbidite sequence in a foreland basin system (Astini, 2003, 2008 and references therein).

In the Huaytiquina section located in the western belt of the Argentine Puna (Fig. 1b), the oldest deposits (900 m thick) correspond to the Aguada de la Perdíz Formation (Puna Volcanic Complex *sensu* Zimmermann, 2011) which is composed of volcanic andesitic breaches, andesitic lava flows, and riolitic-andesitic pyrocalstics (Monteros *et al.*, 1996) (Fig. 3a). More recently, Toro and Herrera Sánchez (2019) and Toro *et al.* (2020) recognized the presence of the *Azygograptus lapworthi* (Dp1) and "*Isograptus victoriae*" (Dp2) biozones, in the middle part of this section, by the occurrence of key graptolites, and conodonts in deposits corresponding to the "Coquena" Formation (Puna Turbidite Complex *sensu* Zimmermann, 2011) (1450 m thick) (Fig. 3a). This unit is unconformably overlain by the Balbuena Sg. (Yacoraite Formation), which, in turn, is unconformably covered by Cenozoic red sandstones with intercalated shales (Monteros *et al.*, 1996). The paleogeographic analysis of the Salta Group (Salfity and Marquillas, 1994) shows that during the start of the accumulation in

the western Puna, a positive structure -Alto de Huaytiquina- was located to the west of the Sey subbasin. For this reason, the *syn-rift* deposits of the Pirgua Sg. were not accumulated. That structure was overflooded in the *post-rift* stage, allowing the Balbuena, and Santa Barbara subgroups to accumulate on the Paleozoic basement and extend towards the Chilenian Terrain (Marquillas and Matthews, 1996). The stratigraphic framework in the area ends with the Cenozoic volcanic and Quaternary deposits (Monteros *et al.*, 1996).

In the Muñayoc section, eastern Puna (Fig. 1b), Toro and Herrera Sánchez (2019) and Lo Valvo *et al.* (2020: fig. 2) recognized four graptolite biozones (*T. akzharensis*, *B.* cf. *B. deflexus*, *D. bifidus*, and *A. lapworthi*) in deposits corresponding to the CEMSC (*sensu* Coira *et al.*, 2004). The stratigraphic sequence reaching 153 m thick overlies the peperites representative of the Ordovician submarine volcanism (Coira *et al.*, 2004) (Fig. 3b). At the top of this section, an angular unconformity separates the CEMSC from deposits of the Balbuena Sg. (Starck, 2011: fig. 2).

A high-resolution correlation of the mentioned localities from the Puna region with the classical localities from the western flank of the Argentine Cordillera Oriental was recently proposed based on graptolite-conodont biostratigraphic analysis (Toro and Herrera Sánchez, 2019; Herrera Sánchez *et al.*, 2019; Toro *et al.*, 2020).

Figure 3. Stratigraphic sections from the Argentine Puna (size: 1.5-column)

8. SAMPLING AND METHODS

3.1 Samples

A total of 14 samples were collected from Northwestern Argentina, with seven samples from the Los Colorados area (Fig. 1b), the Cordillera Oriental, corresponding to the Acoite, and Lipeón formations (Fig. 2). Another seven samples were collected

from the Huaytiquina and Muñayoc areas (Fig. 1b) in the Puna highland and were previously assigned to the "Coquena" Formation (Fig. 3a) and the CEMSC (Fig. 3b), respectively. For identifying the graptolite taxa listed in Figure 4, the reviewed taxonomy presented in the *Treatise of Invertebrate Paleontology* (Maletz *et al.*, 2018a-b) was used. The biostratigraphic discussions are based on the Ordovician graptolite framework successively proposed by Toro (1994, 1997), Toro and Maletz (2007), Toro and Vento (2013), Toro *et al.* (2015), Toro and Herrera Sánchez (2019), and recently summarized by Herrera Sánchez *et al.* (2019) and Toro *et al.* (2020). The proposal of Bergström *et al.* (2009) for referring to the graptolite ages, regional correlations, and global stages was followed.

Figure 4. Table with the provenance and taxonomy of the graptolite samples (size: 2-column)

3.2 Rock-Eval analysis

For the Rock-Eval pyrolysis/TOC analysis, the Rock-Eval 7S instrument was used to determine the parameters shown in Table 1. The analysis was performed using the Basic/Bulk-Rock method (full cycle of pyrolysis and oxidation). The standard used was IFP 160000. Approximately 60 mg of sample powder were placed inside crucibles. The samples were pyrolyzed to measure the contained hydrocarbons as well as CO_2 and CO via a flame ionization detector (FID), and IR cells, respectively. The pyrolysis temperature was initiated at 300 °C isothermal for 3 minutes and increased gradually at a rate of 25 °C/min until 650 °C. For determining the oxidized mineral carbon, and residual carbon, the oxidation oven temperature was 300 °C isothermal for 30 s, and increased gradually by 25 °C/min until 850 °C, and held for 5 min at 850 °C.

3.3 Microscopy

Samples were prepared under the standard method (ISO 7404-2, 2009). The graptolite random reflectance (%GRo) was determined under plane-polarized light using a Zeiss Axio Imager A2m reflected light microscope equipped with a photometer, following ISO 7404-5 (2009) and ASTM D7708-14 (2014) methods. The equivalent vitrinite reflectance (%VRo-eq) was calculated from the mean random graptolite reflectance using the equation established by Petersen *et al.* (2013) (%VRo-eq= [GRo*0.73] +0.16). The paleotemperature "Peak Temperature" (Tpeak) was calculated under "normal" geothermal gradient conditions (Tpeak= [lnVRo-eq+1.68]/0.0124), and hydrothermal conditions (Tpeak-hy= [lnVRo-eq+ 1.19]/0.0782) following Barker and Pawlewicz (1994), and Hartkopf-Fröder *et al.* (2015). Graptolites were identified by their granular or non-granular texture (Goodarzi, 1984; Goodarzi and Norford, 1987) and morphology (Teichmüller, 1978).

All the measurements of the Rock-Eval analysis, graptolite Ro, vitrinite Ro-eq, and calculated paleotemperatures are shown in Tables 1 and 2. The Tpeak values shown in Table 2 are associated with CAI values taken from the literature (Carlorosi *et al.*, 2013; Toro *et al.*, 2020).

3.4 Basin Modeling

To test the results about the burial and thermal history of the Central Andean Basin, based on the graptolite reflectance data for Northwestern Argentina, the PetroMod 1D Express Basin Modeling (from IES GmbH, Schlumberger) was used. For this modeling, the geodynamical approaches explained in the geological framework of this work were considered. The PetroMod software runs numerical simulations involving parameters from each stratigraphic interval such as thickness, lithology, and age, defined depositional and erosional events, and fixing paleowater depth (PWD), seawater interface temperature (SWI), and heat flow (HF) values. Variations in sea

water depth over time could be assumed to be irrelevant because thermal evolution is mainly affected by sediment thickness rather than the depth of the water; SWI is ~21.44 °C. The HF trend was estimated from the typical values associated with different types of sedimentary basins summarized by Allen and Allen (2005: fig. 9.39). Besides, the regional assumptions of Ege *et al.* (2007), and Moretti *et al.* (1996) for the Cenozoic and current values were considered. The specific heat flows used are: Ordovician retro-arc basin (477 My), 70 mW/m^2; collisional event-"Chanic Phase" (359 My), 70 mW/m^2; Cretaceous *rift* event (130 My), 90 mW/m^2; *post-rift* event (60 My), 65 mW/m^2; Early Oligocene exhumation (30 My), 55mW/m^2; at present-day (0 My), 65 mW/m^2. The thickness of the Pirgua, and Balbuena Sg. (Yacoraite Formation) were taken from the Tres Cruces section (Rubiolo *et al.*, 2003; Marquillas *et al.*, 2005).

9. RESULTS AND DISCUSSION

4.1 Rock-Eval pyrolysis, and Total Organic Carbon (TOC)

Rock-Eval/pyrolysis and TOC data for the sections are shown in Table 1. TOC content was very low, ranging from 0.15 to 0.50 wt% in the suite from the Cordillera Oriental, and from 0.09 to 0.90 wt% in the suite from Puna. The S1 values were less than 1.0 mg HC/g rock, except for sample LC-10+12 m (1.88). The S2 values were also very low (<0.36 mg HC/g rock), except for sample LC-10+12 m (1.30). As a result of the very low S2 values, the Tmax values are unreliable and should be discarded. The same applies to the calculated parameters, such as HI, OI, and PI. Rock-Eval pyrolysis data will not be discussed further. The level of thermal maturity was determined by measuring the graptolite reflectance, as will be discussed later.

It is interesting to note that the large difference in thermal maturity between samples retrieved from the LC and MU groups masks their differences in TOC. With an

average of 0.74 wt% the TOC of the samples from MU is nearly three times larger than the TOC of samples in the LC group whose TOC is on average 0.28 wt%. This might reflect a higher amount of deposited organic matter or/and its better preservation in the depositional setting where samples of MU were deposited compared to samples collected in LC.

Table 1. Rock-Eval pyrolysis results

4.2 Age and optical characteristics of the graptolites

The graptolite-bearing samples were collected from three outcropping sections in which the *Tetragraptus akzharensis*, *Baltograptus* cf. *B. deflexus*, *Didymograptellus bifidus*, *Azygograptus lapworthi*, and "*Isograptus victoriae*" biozones were developed (Figs. 2-3), indicating an Early Floian (Fl1) to Early Dapingian (Dp2) age. Besides, the samples that originated from the Lipeón Formation were assigned to the *Stimulograptus sedgwickii* Biozone, which indicates an Aeronian (Early Silurian) age (Toro, 1995) (Fig. 2). The recognized graptolite taxa are listed in Figure 4, which also includes the provenance of the samples.

The graptolite fragments were identified based on morphological features such as the tubarium structure (Figs. 5a-d), common canal, thecae, and thecal branching (Fig. 6c; Figs. 7e-f). The structure corresponds to fine bright and dark lamellar layers on the fusellar tissue (Figs. 5e-f). The graptolites from the Puna region, which are preserved in shales (Muñayoc section; *sensu* Martínez *et al.*, 1999) and calcareous sandstones (Huaytiquina section; *sensu* Toro *et al.*, 2020) are non-granular (Figs. 5a-f; Figs. 6a-f; Fig. 7a). On the other hand, the zooclast fragments from the Los Colorados section, Cordillera Oriental, were poorly preserved and fragmented, and were encountered mostly normal to the bedding plane, and had a pitted texture (Figs. 7b-d).

The lower reflectance and weaker anisotropy of graptolites from the Cordillera Oriental region (Table 2) indicate their low maturity. On the other hand, the graptolite fragments from the Muñayoc, and Huaytiquina sections in Puna are high-reflecting, pointing to considerably higher maturity.

Table 2. Graptolite, and equivalent vitrinite reflectance, Tpeak

Figures 5, 6, and 7. Graptolites under reflected light (size: 2-column each one)

4.3 Graptolite reflectance and thermal maturity of Paleozoic rocks from Northwestern Argentina

Graptolite random reflectance measurements from the Los Colorados section range from 0.63%-1.11% (Table 2) with corresponding VRo-eq between 0.62% to 0.97% (Table 2), indicating that the organic matter is between the early to the peak stages of the oil window, corresponding to the catagenetic stage (*sensu* Abad, 2007). The reflectance histograms of the six samples analyzed from the above section are displayed in Figure 8 (a-f). The calculated Tpeak values in the range of 97 °C-133 °C reflect the maximum burial depth experienced by the graptolites in this section and agree with the temperature estimated from the 1.5-2 CAI of conodonts from the Lower Member of the Alto del Cóndor Formation (Carlorosi *et al.*, 2013), which is approximately 100 °C. One sample (LC-10+12 m) did not contain any measurable graptolite fragments. The eastern basin, which coincides with the present-day Cordillera Oriental, did not experience synsedimentary magmatic activity, so the thermal parameters measured in this work could indicate the maximum depth of burial. The three higher Tpeak values (119, 122, and 133 °C) corresponding to the graptolites in samples LC-17, LC-21, and LC-24+40m could reflect some influence of hydrothermal activity.

Figure 8. Histograms (size: 2-columns)

On the other hand, the graptolite random reflectance in the Argentine Puna region is 6.15% in the Huaytiquina section and varies between 5.57%-6.62% in the Muñayoc area (Table 2). The equivalent vitrinite reflectance in the Argentine Puna ranges from 4.23%-4.99% (Table 2), and Tpeak varies from 252 °C to 265 °C, indicating post-mature organic matter (dry gas stage) and consistent with an epizone metapellitic zone (*sensu* Abad, 2007). Furthermore, graptolite fragments having considerably higher reflectance, from 8.8-10.1%, were measured (Table 2), corresponding to VRo-eq of 6.5-7.5%, and temperatures above 300 ^{o}C. These graptolites exhibited strain anisotropy, although the fusinal layer structure was still visible when the analyzer was inserted (Fig. 5f). These very high %Ro values of graptolites affected by tectonic activity were not used to model the level of thermal maturity in the Puna region.

The common occurrence of kaolinite in the slates of the Cochinoca-Escaya Range in the Puna region, coupled with the substitution of chlorite by interstratified lower-temperature phases in most of these rocks, and the occurrence of jarosite in a metadacite indicate the presence of hydrothermal fluids with high H^{+}/cation ratios. These fluids can produce acid-type alteration at temperatures between 100 $^{\circ}$C and ~300 °C (Do Campo *et al.*, 2017). Besides, the Ordovician rocks in this study are related to mineralized quartz veins, gold-bearing “saddle reefs” with As, Fe, Cu, Pb, Zn, Sb sulfides, and sulfosalts of silver in the Cochinoca-Escaya, and Rinconada ranges (Craig *et al.*, 1995; Coira *et al.*, 2001). Likewise, Coira *et al.* (2004) recognized concentrations of pyrite crystals with the development of pressure forms filled with neoformed phyllosilicates, probably the product of hydrothermal alteration, in the pelitic facies of the CEMSC.

For these reasons, the data presented in this work provides an estimate of the temperature of the hydrothermal fluids, which ranges from 336 °C to 358 °C in the Puna region (Table 2). Such values are close to the maximum temperatures estimated by Do Campo *et al.* (2017), which explains the highest measured random reflectance values measured on three graptolite tubaria collected at the Puna region (%GRo~10-11%). The above temperatures are so high that they are beyond dry gas (methane) generation or retention. The strain anisotropy exhibited by the graptolites in this region (Figs. 5e-f) is characteristic of organic matter found in orogenic belts that have experienced tectonic deformation such as thrusting and folding (Goodarzi and Norford, 1985). The "Ocloyic Phase" and Central Andes uplift had a considerable impact on the very high reflectance and strain anisotropy attained by the graptolites collected from the Argentine Puna. Besides, in the present-day Puna region, the deposits assigned to Tremadocian-Dapingian ages contain abundant intercalated volcaniclastics rocks (Bahlburg, 1990; Zimmermann and Balhburg, 2003; Zimmermann, 2011), which points to intense magmatic activity during deposition (Mon and Salfity, 1995). The very high thermal maturity of the graptolites in the Puna region could be explained by combined effect of higher geothermal gradients associated with the synsedimentary volcanism, hydrothermal fluids, as well as tectonism, i.e., during the Ocloyic Orogeny, and Central Andes uplift.

The 1.5-2 CAI value of conodonts from the Huaytiquina section (Toro *et al.*, 2020), which correspond to ~100 °C of the Epstein *et al.* (1977) table, does not coincide with the paleotemperature obtained from the reflectance measurements (i.e., sample RH-A, Table 2) that indicate temperatures greater than 300 °C. This is most likely due to the thermal effect of hydrothermal fluids on the graptolite organic matter, which is more sensitive to temperatures than fluorapatite, especially in overmatured sediments

(Goodarzi and Norford, 1985). The temperatures of 300 ^{o}C are in agreement with those estimated by the CAI values of 4-5 of the conodonts in the Salar del Rincón area in southern Puna (Do Campo *et al.*, 2017). However, the correlation between graptolite reflectance and CAI values greater than 4-5 is not clear (Goodarzi and Norford, 1985; Goodarzi *et al.*, 1992; Luo *et al.*, 2020) and should be treated with caution.

As a consequence of the hydrothermal effect associated with volcanism (Astini, 2003; Zimmermann and Bahlburg, 2003; Coira *et al.*, 2004; Zimmermann, 2011; Do Campo *et al.*, 2017 and references therein), the graptolite reflectance, and accordingly the equivalent vitrinite reflectance do not indicate the maximum depth of burial of the "Coquena" Formation, and CEMSC strata in the Argentine Puna region north of 24^{o} S latitude.

4.4 Thermal maturity modeling: preliminary comments

Several thermal models were carried out with PetroMod to test the thermal conditions for the Central Andean Basin only at the Los Colorados section, Cordillera Oriental, because other studied sections from the Puna region are probably altered by hydrothermal fluids and volcanic intrusives. The thermal evolution of the basin was reconstructed under five different conditions (Fig. 9): a) considering a complete Cretaceous and Cenozoic succession overlying the Paleozoic sequence taken as reference the thickness of the Tres Cruces section (>3500 m); b) considering that during 358-130 My, after the "Chanic Phase", a thickness of ~3000 m were deposited in Los Colorados area as occurred in the Sierras Subandinas belt (*sensu* Starck, 1995); c) considering that is probably that the Argentine Cordillera Oriental was emerged between 358-130 My, and ~900 m were eroded after the "Chanic Phase"; d) considering that ~265 m were eroded since 38 My until now as a product of the Central Andes uplift; e) considering c, and d in the same input data.

As shown in Figure 9a, vitrinite reflectance at the middle part of the Acoite Formation (at ~8500 m depth) considering a complete Cretaceous and Cenozoic succession overlying the Paleozoic sequence is about 4.55%. This high trending in VRo also occurs when a thickness of ~3000 m deposited between 358-130 My was considered. In this case, vitrinite reflectance measurement is 4.55% at ~7500 m depth (Fig. 9b). In both models, reflectance values exceed the obtained VRo-eq in this work (Table 2). On the other hand, in the alternative where ~900 m were eroded between 358-130 My, vitrinite reflectance is 1.10% at ~2200 m depth (Fig. 9c). Meanwhile, when a thickness of ~265 m was eroded during the Central Andes uplift in the latest 38 My, VRo at the middle part of the Acoite Formation is about 1.40% at ~2200 m depth (Fig. 9d). The latest alternative is considering options c and d in the same input data. In this case, vitrinite reflectance is 0.97% at ~2200 m depth (Fig. 9e). This approach considering erosion episodes at the Late Paleozoic and Early Cenozoic seems to fit with the geothermal parameters (VRo-eq) measured in this work (Table 2), which ranges between 0.80%-1.00% at the middle part of the Acoite Formation, and could explain the evolution of the Los Colorados section. This model agrees with the hypothesis that part of the Argentine Cordillera Oriental remains emerged between the Late Devonian and Early Cretaceous, which explain the scarce Siluro-Devonian strata (Starck, 1995). The deposits eroded at this time (~900 m) would probably be part of the Cinco Picachos Supersequence (Zapla, Lipeón, Baritú=Arroyo Colorado, and Porongal formations) that reaches more than 2000 m thick in the Cinco Picachos Range along the boundary between the Cordillera Oriental, and Sierras Subandinas belt (*sensu* Starck, 1995). On the other hand, also it is probably that the Los Colorados area was an emerged zone since 38 My when the Cordillera Oriental started to uplift as a consequence of the development of the Central Andes (*sensu* Coutand *et al.*, 2001), producing the erosion

of ~265 m of the Yacoraite Formation until now. However, more studies about geothermal parameters and stratigraphy for Northwestern Argentina are necessary to corroborate these preliminary models, and propose new approaches for the Puna region.

Figure 9. Thermal maturity modeling (size: 2-column)

10. CONCLUSIONS

Graptolite reflectance can be used to determine the level of maturity of organic matter, but other factors such as hydrothermal fluid activity, magmatism, and tectonism can alter the results and the interpretations.

The VRo-eq values calculated from the mean random reflectance of the graptolites from the Los Colorados section, Cordillera Oriental, range from 0.62%-0.97% with corresponding Tpeaks of 97°C and 133°C. These values place the organic matter in the oil window (early to middle part) and reflect the shallow burial depth of the graptolite-bearing interval in this area of the Central Andean Basin.

The high graptolite reflectance values from the Puna region between 5.57%-6.62% and corresponding VRo-eq between 4.23%-4.99% place the organic matter in the post-mature stage (even beyond dry methane gas generation/presentation). Such a high maturity could be the result of the combined effects of hydrothermal fluids, higher geothermal gradient associated with volcaniclastics, and deformation from tectonics events. The latter resulted in the high strain anisotropy of the graptolites.

The results presented in this work are in agreement with the trend proposed by Do Campo *et al.* (2017), which reflects higher temperatures (high anchizone/epizone) in the Puna region than those obtained for the Cordillera Oriental (catagenesis/low anchizone). It is also coincident with the proposed location of the Ocloyic deformation belt.

Modeling considering erosion episodes at Late Paleozoic and Early Cenozoic seems to fit with the geothermal parameters (VRo-eq) measured in this work, which ranges between 0.80%-1.00% at the middle part of the Acoite Formation, and could explain the evolution of the Los Colorados section. However, more studies about geothermal parameters and stratigraphy are necessary to corroborate these preliminary models, and propose new approaches for the Puna region.

ACKNOWLEDGEMENTS

We would like to thank the editor, Prof. Deolinda Flores, for her expedient and professional manner she handled our manuscript and the two anonymous reviewers for offering valuable comments and suggestions, which resulted in the improvement of the manuscript. N.C.H.S. thanks to M. Ezpeleta for providing information about the software to reproduce the thermal maturity model. This work was supported by the Agencia Nacional de Promoción Científica y Tecnológica (PICT 2016-0558), and Consejo Nacional de Investigaciones Científicas y Técnicas (CONICET). It is a contribution to 653 IUGS-IGCP project -The onset of the Great Ordovician Biodiversification event-, and was developed on the framework of the Ph.D. thesis of the first author (N.C.H.S).

REFERENCES

Abad, I., 2007. Physical meaning and applications of the illite Kübler index: measuring reaction progress in low-grade metamorphism, in: Nieto, F., Jiménez-Millán, J. (Eds.), Diagenesis and low-Temperature Metamorphism, Theory, Methods and Regional Aspects. Sociedad Española: Sociedad Española Mineralogía, pp. 53–64.

Albanesi, G.L., Ortega, G.C., 2016. Conodont and graptolite biostratigraphy of the Ordovician System of Argentina, in: Montenari, M. (Ed.), Stratigraphy & Timescales. Oxford: Elsevier Inc, pp. 61–121.

Allen, P.A., Allen, J.R., 2005. Basin analysis: Principles and Applications. Blackwell Scientific Publications, Oxford.

Aparicio González, P., Uriz, N., Arnol, J., Martínez Dopico, C., Cayo, L.E., Cingolani, C., Impiccini, A., Stipp Basei, M.A., 2020. Sedimentary provenance analysis of the ordovician to devonian siliciclastic units of the Subandean Ranges and Santa Barbara System, northwestern Argentina. Journal of South American Earth Sciences, https://doi.org/10.1016/j.jsames.2020.102629

ASTM Standard D7708-14., 2014. Standard Test Method for Microscopical Determination of the 593 Reflectance of Vitrinite Dispersed in Sedimentary Rocks. ASTM International, West 594 Conshohocken, PA.

Astini, R.A., 1999. Sedimentary record, volcano-tectonic cyclicity and progressive emergence of an Early Ordovician perigondwanic volcanic arc: The Famatinian System, in: Fraft, P., Fatka, O. (Eds.), Quo vadis Ordovician?. Acta-Universitatis Carolinae Geologica (1-2), pp. 115–118.

Astini, R.A., 2002. Los conglomerados basales del Ordovícico de Ponón Trehue (Mendoza) y su significado en la historia sedimentaria del terreno exótico de Precordillera. Revista de la Asociación Geológica Argentina 57, 19–34.

Astini, R.A., 2003. Ordovician Basins of Argentina, in: Benedetto, J.L. (Ed.), Ordovician fossils of Argentina. Secretaría de Ciencia y Tecnología, Universidad Nacional de Córdoba, pp. 1–74.

Astini, R.A., 2008. Sedimentación, facies discordancias y evolución paleoambiental durante el Cambro–Ordovícico, in: Coira, B., Zappetteni, E.O. (Eds.). Geología y

recursos naturales de la provincia de Jujuy, Relatorio del 17° Congreso Geológico Argentino, Buenos Aires: Asociación Geológica Argentina, pp. 50–73.

Astini, R.A., Waisfeld, B.G., Toro, B.A., Benedetto, J.L., 2004. El Paleozoico inferior y medio de la región de Los Colorados, borde occidental de la Cordillera Oriental (Provincia de Jujuy). Revista de la Asociación Geológica Argentina 59, 243–260.

Astini, R.A., Coppa Vigliocco, A., Gómez, F.J., 2019. Una cuña marina dominada por mareas en la base de la Formación Lecho en el extremo noroeste argentino. Revista de la Asociación Geológica Argentina 77 (2), 271–295.

Bahlburg, H., 1990. The Ordovician basin in the Puna of NW Argentina and N Chile: geodynamic evolution from back-arc to foreland basin. Geotektonische Forschungen 75, 1–107.

Bahlburg, H., Hervé, F., 1997. Geodynamic evolution and tectonostratigraphic terranes of northwestern Argentina and northern Chile. GSA Bulletin 109 (7), 869–884.

Barker, C.E., Pawlewicz, M.J., 1994. Calculation of vitrinite reflectance from thermal histories and peak temperatures. A comparison of methods, in: Mukhopadhyay, P. K., Dow, W.G. (Eds.), Vitrinite Reflectance as a Maturity Parameter: Applications and Limitations. ACS Symposium Series 570, pp. 216–229.

Bergström, S.M., Chen, X., Gutiérrez-Marco, J.C., Dronov, A., 2009. The new chronostratigraphic classification of the Ordovician System and its relations to major regional series and stages to δ13C chemostratigraphy. Lethaia 42 (1), 97–107.

Boll, A., Hernandez, M., 1986. Interpretación estructural del área de Tres Cruces. Boletín de Informaciones Petroleras, Tercera Época, Año III, 7, 2–14.

Brussa, E.D., Toro, B.A., Vaccari, N.E., 2008. Bioestratigrafía del Paleozoico inferior en el ámbito de la Puna, in: Coira, B., Zappetteni, E.O. (Eds.), Geología y recursos

naturales de la provincia de Jujuy, Relatorio del 17° Congreso Geológico Argentino, Buenos Aires: Asociación Geológica Argentina, pp. 93–97.

Buatois, L.A., Mángano, M.G., Moya, M.C., 2000. Incisión de valles estuarinos en el Cámbrico Tardío del noroeste argentino y la problemática del límite entre los grupos Mesón y Santa Victoria. Segundo Congreso Latinoamericano de Sedimentología, Resúmenes, 55.

Buatois, L.A., Mángano, M.G., 2003. Sedimentary facies, depositional evolution of the Upper Cambrian - Lower Ordovician Santa Rosita formation in northwest Argentina. Journal of South American Earth Sciences 16, 343–363.

Carlorosi, J., Heredia, S., Aceñolaza, G., 2013. Middle Ordovician (Early Dapingian) conodonts in the Central Andean Basin of NW Argentina. Alcheringa 37 (3), 299–311.

Casquet, C., Dahlquist, J.A., Verdecchia, S.O., Baldo, E.G., Galindo, C., Rapela, C.W., Pankhurst, R.J., Morales, M.M., Murra, J.A., Mark Fanning, C., 2018. Review of the Cambrian Pampean orogeny of Argentina; a displaced orogen formerly attached to the Saldania Belt of South Africa?, Earth-Science Reviews 177, 209–225.

Coira, B., 2008. Volcanismo del Paleozoico inferior en la Puna Jujeña, in: Coira, B., Zappetteni, E.O. (Eds.), Geología y recursos naturales de la provincia de Jujuy, Relatorio del 17° Congreso Geológico Argentino, Buenos Aires: Asociación Geológica Argentina, pp. 267–292.

Coira, B., Caffe, P.J., Ramírez, A., Chayle, W., Díaz, A., Rosas, S., Pérez, A., Pérez, E.M.B., Orozco, O., Martínez, M., 2001. Hoja Geológica 2366-I/2166-III “Mina Pirquitas”, Provincia de Jujuy. Servicio Geológico Minero Argentino, Instituto de Geología y Recursos Minerales, Boletín 269.

Coira, B., Caffe, P.J., Ramírez, A., Chayle, W., Díaz, A., Rosas, S., Pérez, A., Pérez, E.M.B., Orozco, O., Martínez, M., 2004. Hoja Geológica 2366-I/2166-III Mina Pirquitas, Provincia de Jujuy (escala 1:250.000). Servicio Geológico Minero Argentino, Instituto de Geología y Recursos Minerales, Boletín 269.

Cole, G.A., 1994. Graptolite-chitinozoan reflectance and its relationship to other geochemical maturity indicators in the Silurian Qusaiba Shale, Saudi Arabia. Energy Fuel 8, 1443–1459.

Coutand, I., Cobbold, P.R., de Urreiztieta, M., Gautier, P., Chauvin, A., Gapais, D., Rosello, E. A., López-Gamundí, O., 2001. Style and history of Andean deformation, Puna plateau, northwestern Argentina. Tectonics 20 (2), 210–234.

Craig, J.R., Segal, S.J., Zappettini, E.O., 1995. El distrito aurífero Rinconada, Provincia de Jujuy, República Argentina. Congreso Latinoamericano de Geología, No. 10, Actas 2, 22–35.

Dalenz-Farjat, A., Alvarez, L.A., Hernández, R.M., Albariño, L.M., 2002. Cuenca Siluro-Devónica del sur de Bolivia y del noroeste argentino: algunas interpretaciones. Congreso de Exploración y Desarrollo de Hidrocarburos, No. 5, 222–248.

Do Campo, M., Nieto, F., Albanesi, G.L., Ortega, G., Monaldi, R., 2017. Outlining the thermal posdepositional evolution of the Ordovician successions of northwestern Argentina by clay mineral analysis, chlorite geothermometry and Kübler index. Andean Geology 44 (2), 179–212.

Ege, H., Sobel, E.R., Scheuber, E., Jacobshagen, V., 2007. Exhumation history of the southern Altiplano plateau (southern Bolivia) constrained by apatite fission track thermochronology. Tectonics 26 (1), 1–24, TC1004.

Egenhoff, S.O., 2007. Life and death of a Cambrian–Ordovician basin: An Andean three-act play featuring Gondwana and the Arequipa-Antofalla terrane. Geological Society of America Special Papers 423, 511–524.

Epstein, A.G., Epstein, J.B., Harris, L.D., 1977. Conodont color alteration–an index to organic metamorphism. Geological Survey Professional Paper 995, 1–27.

Escayola, M.P., van Staal, C.R., Davis, W.J., 2011. The age and tectonic setting of the Puncoviscana Formation in northwestern Argentina: An accretionary complex related to Early Cambrian closure of the Puncoviscana Ocean and accretion of the Arequipa-Antofalla block. Journal of South American Earth Sciences 32 (4), 438–459.

Fernández, R., Guerrero, C., Manca, N., 1982. El límite Cámbro-Ordovícico en el tramo medio y superior de la quebrada de Humahuaca, Provincia de Jujuy, Argentina. 5to Congreso Latinoamericano de Geología, Actas 1, 3–22.

Forsythe, R.D., Davidson, J., Mpodozis, C., Jesinkey, C., 1993. Lower Paleozoic relative motion of the Arequipa Block and Gondwana; Paleomagnetic evidence from Sierra de Almeida of northern Chile. Tectonics 12 (1), 219–236.

Gentzis, T., de Freitas, T., Goodarzi, F., Melchin, M., Lenz, A., 1996. Thermal maturity of Lower Paleozoic sedimentary successions in Arctic Canada. American Association of Petroleum Geologists Bulletin 80, 1065–1084.

Gohrbandt, K.H.A., 1992. Paleozoic paleogeographic and depositional developments on the central proto-Pacific margin of Gondwana: Their importance to hydrocarbon accumulation. Journal of South American Earth Sciences 6 (4), 267–287.

González, M.A., Pereyra, F., Ramallo, E., Tchilinguirian, P., 2003. Hoja Geológica 2366-IV, Ciudad de Libertador General San Martín, provincias de Jujuy y Salta.

Instituto de Geología y Recursos Minerales, Servicio Geológico Minero Argentino, Boletín 274.

Goodarzi, F., 1984. Organic petrography of graptolite fragments from Turkey. Marine and Petroleum Geology 1, 202–210.

Goodarzi, F., 1985. Reflected light microscopy of chitinozoan fragments. Marine and Petroleum Geology 2, 72–78.

Goodarzi, F., Norford, B., 1985. Graptolites as indicators of the temperature histories of rocks. Journal of the Geological Society 142, 1089–1099.

Goodarzi, F., Higgins, A.C., 1987. Optical properties of scolecodonts and their use as indicators of thermal maturity. Marine and Petroleum Geology 14, 353–359.

Goodarzi, F., Norford, B., 1987. Optical properties of graptolite epiderm–a review. Bulletin of the Geological Society of Denmark 35, 141–147.

Goodarzi, F., Norford, B., 1989. Variation of graptolite reflectance with depth of burial. International Journal of Coal Geology 11, 127–141.

Goodarzi, F., Stasiuk, L.D., Lindholm, K., 1988. Graptolite reflectance and thermal maturity of Lower and Middle Ordovician shale from Scania, Sweden. Geologiska Föreningen i Stockholm Förhandlingar 110 (3), 225–236.

Goodarzi, F., Fowler, M.G., Bustin, M., McKirdy, D.M., 1992a. Thermal maturity of Early Paleozoic sediments as determined by the optical properties of marine–derived organic matter–A Review. Early Organic Evolution, 279–295.

Goodarzi, F., Gentzis, T., Harrison, J.C., Thorsteinsson, R., 1992b. The significance of graptolite reflectance in regional thermal maturity studies, Queen Elizabeth Islands, Arctic Canada. Organic Geochemistry 18, 347–357.

Grahn, Y., Gutierrez, P.R., 2001. Silurian and Middle Devonian Chitinozoa from the Zapla and Santa Barbara Ranges, Tarija Basin, northwestern Argentina. Ameghiniana 38, 35–50.

Hao, J., Zhong, N., Luo, Q., Dehan, L., Wu, J., Liu, A., 2019. Raman spectroscopy of graptolite periderm and its potential as an organic maturity indicator for the Lower Paleozoic in southwestern China. International Journal of Coal Geology 213, https://doi.org/10.1016/j.coal.2019.103278

Hartkopf-Fröder, C., Königshof, P., Littke, R., Schwarzbauer, J., 2015. Optical thermal maturity parameters and organic geochemical alteration at low grade diagenesis to anchimetamorphism: a review. International Journal Coal Geology 150–151, 74–119.

Herrera Sánchez, N.C., Toro, B.A., Lo Valvo, G.A., 2019. Lower–Middle Ordovician graptolite biostratigraphy and future challenges for the Central Andean Basin (NW Argentina and S Bolivia), in: Obut, O.T., Sennikov, N.V., Kipriyanova, T.P. (Eds.), Contributions of the 13th International on the Ordovician System. Novosibirsk: Publishing House of SB RAS, pp. 71–74.

Hongn, F.D., Vaccari, N.E., 2008. La discordancia Tremadociano superior-Arenigiano inferior en Vega Pinato (Salta): Evidencia de deformación intraordovícica en el borde occidental de la Puna, in: Coira, B., Zappetteni, E.O. (Eds.), Geología y recursos naturales de la provincia de Jujuy, Relatorio del 17° Congreso Geológico Argentino, Buenos Aires: Asociación Geológica Argentina, pp. 1299–1300.

İnan, S., Goodarzi, F., Mumm, A.S., Arouri, K., Qathami, S., Ardakani, O.H., İnan, T., Tuwailib, A.A., 2016. The Silurian Qusaiba Hot Shales of Saudi Arabia: an integrated assessment of thermal maturity. International Journal of Coal Geology 159, 107–119.

ISO 7404-2., 2009. Methods for the Petrographic Analysis of Coals - Part 2: Methods of Preparing Coal Samples. International Organization for Standardization, 1–12.

ISO 7404-5., 2009. Methods for the Petrographic Analysis of Coals - Part 5: Method of Determining Microscopically the Reflectance of Vitrinite. International Organization for Standardization, 1–14.

Jacobshagen, V., Müller, J., Wemmer, K., Ahrendt, H., Manutsoglu, E., 2002. Hercynian deformation and metamorphism in the Cordillera Oriental of Southern Bolivia, Central Andes. Tectonophysics 345, 119–130.

Kley, J., Reinhardt, M., 1994.Geothermal and tectonic evolution of the Eastern Cordillera and the Subandean Ranges of Southern Bolivia, in: Reutter, K.J., Scheuber, E., Wigger, P.J. (Eds.), Tectonics of the Southern Central Andes. Structure and Evolution of an Active Continental Margin. Springer Verlag, pp. 155–170.

Kurylowicz, L., Ozimic, S., Mckirdy, D., Kantsler, A., Cook, A., 1976. Reservoir and source rock potential of the Larapinta Group, Amadeus Basin, central Australia. Australian Petroleum Exploration Association Journal 16, 49–65.

Lo Valvo, G.A., Herrera Sánchez, N.C., Toro, B.A., 2020. Early-Middle Ordovician graptolites from the Argentine Puna: quantitative paleobiogeographic analysis based on a systematic revision. Ameghiniana 57 (6), 534–554.

Luo, Q., Zhong, N., Dai, N., Zhang, W., 2016. Graptolite-derived organic matter in the Wufeng–Longmaxi Formations (Upper Ordovician–Lower Silurian) of southeastern Chongqing, China: implications for gas shale evaluation. International Journal of Coal Geology 153, 87–98.

Luo, Q., Hao, J., Skovsted, C.B., Luo, P., Khan, I., Wu, J., Zhong, N., 2017. The organic petrology of graptolites and maturity assessment of the Wufeng–

Longmaxi Formations from Chongqing, China: Insights from reflectance cross-plot analysis. International Journal of Coal Geology 183, 161–173.

Luo, Q., Hao, J., Skovsted, C.B., Xu, Y., Liu, Y., Wu, J., Zhang, S., Wang, W., 2018. Optical characteristics of graptolite-bearing sediments and its implication for thermal maturity assessment. International Journal of Coal Geology 195, 386–401.

Luo, Q., Goodarzi, F., Zhong, N., Wang, Y., Qiu, N., Skovsted, C., Suchý, V., Hemmingsen Schovsbo, N., Morga, R., Xu, Y., Hao, J., Liu, J., Wu, J., Cao, W., Min, X., Wu, J., 2020. Graptolites as fossil geo-thermometers and source material of hydrocarbons: an overview of four decades of progress. Earth-Science Reviews 200, https://doi.org/10.1016/j.earscirev.2019.103000

Maletz, J., Lenz, A.C., Bates, D.E., 2016. Part V, Second Revision, Chapter 4: Morphology of the Pterobranch Cubarium. Treatise Online 76, 1–63.

Maletz, J., Toro, B.A., Zhang, Y.D., VandenBerg, A.H.M., 2018a. Part V, Second Revision, Chapter 20: Suborder Dichograptina: Introduction, Morphology, and Systematic Descriptions. Treatise Online 108, 1–28.

Maletz, J., Zhang, Y.D., VandenBerg, A.H.M., 2018b. Part V, Second Revision, Chapter 19: Suborder Sinograptina: Introduction, Morphology, and Systematic Descriptions. Treatise Online 107, 1–23.

Mángano, M.G., Buatois, L.A., 2004. Integración de estratigrafía secuencial, sedimentología e icnología para un análisis cronoestratigráfico del Paleozoico inferior del noroeste argentino. Revista de la Asociación Geológica Argentina 59 (2), 273–280.

Martínez, M., Brussa, E.D., Pérez, B., Coira, B., 1999. El Ordovícico de la Sierra de Quichagua (Puna oriental argentina): litofacies volcanosedimentarias y graptofaunas. Actas de 14° Congreso Geológico Argentino, 347–350.

Marquillas, R.A., Matthews, S.J., 1996. Skarn formation beneath Lascar volcano, N Chile: evidence for the western continuation of the Yacoraite Formation (Late Cretaceous) of NW Argentina. III Symposium International sur la Géodynamique Andine, 431–434.

Marquillas, R.A., del Papa, C., Sabino, I.F., 2005. Sedimentary aspects and paleoenvironmental evolution of a rift basin: Salta Group (Cretaceous–Paleogene), northwestern Argentina. International Journal of South American Earth Sciences 94, 94–113.

Mon, R., Hongn, F.D., 1991. The structure of the Precambrian and Lower Paleozoic basement of the Central Andes between 22° and 32° S. Lat. Geologische Rundschau 80, 745–758.

Mon, R., Salfity, J.A., 1995. Tectonic evolution of the Andes of Northern Argentina, in: Tankard, A.J., Suárez, R., Welsink, H.J. (Eds.), Petroleum Basins of South America. American Association of Petroleum Geology, Memoir 62, pp. 269–283.

Mon, R., Hongn, F., 1996. Estructura del basamento proterozoico y paleozoico inferior del norte argentino. Revista de la Asociación Geológica Argentina 51 (1), 3–14.

Monteros, J.A., Moya, M.C., Monaldi, C.R., 1996. Graptofaunas arenigianas el borde occidental de la Puna Argentina. Implicancias paleogeográficas. Memorias del 12° Congreso Geológico de Bolivia 2, 733–746.

Moretti, I., Baby, P., Mendez, E., Zubieta, D., 1996. Hydrocarbon generation in relation to thrusting in the Sub Andean zone from 18 to 22°S, Bolivia. Petroleum Geoscience 2 (1), 17–28.

Moya, M.C., 1998. Lower Ordovician in the southern part of the argentine eastern cordillera, in: Bahlburg, H., Breitkreuz, C., Giese, P. (Eds.), The Southern Central Andes: Contributions to Structure and Evolution of an Active Continental Margin. Springer Berlin Heidelberg, Berlin, Heidelberg, pp. 55–69.

Moya, M.C., 1999. El Ordovícico en los Andes del norte argentino, in: González Bonorino, G., Omarini, R., Viramonte, J. (Eds.), Geología del Noroeste Argentino. Congreso Geológico Argentino, No. 14, Relatorio I, Buenos Aires: Asociación Geológica Argentina, pp. 134–152.

Moya, M.C., 2003. The Ordovician System in the Argentina Eastern Cordillera, in: Ordovician and Silurian of the Cordillera Oriental and Sierras Subandinas, NW Argentina. Field Trip Guide. Instituto Superior de Correlación Geológica (INSUGEO), Serie Correlación Geológica 11, pp. 7–16.

Moya, M.C., 2015. La "Fase Oclóyica" (Ordovícico Superior) en el noroeste argentino. Interpretación histórica y evidencias en contrario. Instituto Superior de Correlación Geológica (INSUGEO), Serie Correlación Geológica 31 (1), 73–110.

Moya, M.C., Monteros, J.C., 1999. El Ordovícico tardío y el Silúrico en el borde Occidental de la Cordillera Oriental Argentina. 14º Congreso Geológico Argentino, Actas 1. Buenos Aires: Asociación Geológica Argentina, 401–404.

Obermayer, M., Fowler, M.G., Goodarzi, F., Snowdon, L.R., 1996. Assessing thermal maturity of Palaeozoic rocks from reflectance of chitinozoa as constrained by geochemical indicators: an example from southern Ontario, Canada. Marine and Petroleum Geology 13, 907–919.

Petersen, H.I., Schovsbo, N.H., Nielsen, A.T., 2013. Reflectance measurements of zooclasts and solid bitumen in Lower Palaeozoic shales, southern Scandinavia:

correlation to vitrinite reflectance. International Journal of Coal Geology 114, 1–18.

Ramos, V., Jordan T., Allmendinger R., Kay S., Cortés J., Palma M., 1984. Chilenia: un terreno alóctono en la evolución paleozoica de los Andes centrales. IX Congreso Geológico Argentino, Buenos Aires: Asociación Geológica Argentina 2, 84–106.

Rubiolo, D., Seggiaro, R., Gallardo, E., Disalvo, A., Sánchez, M., Turel, A., Ramallo, E., Sandruss, A., Godeas, M., 2003. Hoja Geológica 2366-II / 2166-IV, La Quiaca. Provincias de Jujuy y Salta. Servicio Geológico Minero Argentino, Instituto de Geología y Recursos Minerales, Boletín 246.

Ruiz Huidobro, O.J., 1975. El Paleozoico Inferior del centro y sur de Salta y su correlación con el Grupo Mesón. 1er Congreso Argentino de Paleontología y Bioestratigrafía, Actas 1, 91–107.

Salfity, J.A., Marquillas, R.A., 1994. Tectonic and sedimentary evolution of the Cretaceous-Eocene Salta Group Basin, Argentina, in: Salfity, J.A. (Ed.), Cretaceous Tectonics of the Andes. Earth Evolution Sciences, Friedr. Vieweg & Sohn, pp. 266–315.

Sempere, T., 1995. Phanerozoic evolution of Bolivia and adjacent regions, in: Tankard, A.J., Suárez Soruco R., Welsink H.J. (Eds.), Petroleum basins of South America. AAPG Memoir 62, pp. 207–230.

Suárez-Ruiz, I., Flores, D., Mendonça Filho, J.G., Hackley, P.C., 2012. Review and update of the applications of organic petrology: Part 1, geological applications. International Journal of Coal Geology 99, 54–112.

Suchý, V., Sýkorová, I., Stejskal, M., Sâfanda, J., Machovič, V., Novotná, M., 2002. Dispersed organic matter from Silurian shales of the Barrandian Basin, Czech

Republic: optical properties, chemical composition and thermal maturity. International Journal of Coal Geology 53, 1–25.

Starck, D., 1995. Silurian-Jurassic stratigraphy and basin evolution of northwestern Argentina, in: Tankard, A.J., Suárez Soruco R., Welsink H.J. (Eds.), Petroleum basins of South America. AAPG Memoir 62, 251–267.

Starck, D., 2011. Cuenca Cretácica-Paleógena del Noroeste argentino. VIII Congreso de Exploración y Desarrollo de Hidrocarburos Simposio. Cuencas Argentinas: visión actual, Actas, 407–453.

Starck, D., Gallardo, E., Schultz, A., 1992. La discordancia precarbónica en la porción argentina de la Cuenca de Tarija. Boletín de Informaciones Petroleras, Buenos Aires, Argentina, Tercera Época 29, 2–11.

Starck, D., Gallardo, E., Schultz, A., 1993. The pre-Carboniferous unconformity in the Argentine portion of the Tarija Basin. XII International Congress on Carboniferous–Permian 2, 373–384.

Starck, D., Rodriguez, A., Constantini, L., 2002. Los Reservorios de las formaciones Tupambí, Tarija, Las Peñas y San Telmo, in: Schiuma, M., Vergani, G., Hinterwimmer, G. (Eds.): Las rocas reservorio de las cuencas productivas de la Argentina. V Congreso de Exploración y Desarrollo de Hidrocarburos, pp. 699–716.

Tawackoli, S., Kley, J., Jacobshagen, V., 1996. Evolución tectónica de la Cordillera Oriental del sur de Bolivia. Memorias del 12° Congreso Geológico de Bolivia 1, 91–96.

Teichmüller, M., 1978. Nachweis von graptolithen-periderm in geschieferten gesteinen mit hilfe kohlenpetrologischer methoden. Neues Jahrbuch für Geologie und Paläontologie, Monatshefte 7, 430–447.

Toro, B.A., 1993. Graptofauna arenigiana de la Quebrada del río Cajas (Formación Acoite), Provincia de Jujuy, Argentina. Ameghiniana 30 (1), 69–76.

Toro, B.A., 1994. Las zonas de *Didymograptus* (*Didymograptellus*) *bifidus* (Arenigiano medio) y *Didymograptus* (*Corymbograptus*) *deflexus* (Arenigiano inferior) en la Formación Acoite, Cordillera Oriental, Argentina. Ameghiniana 31 (3), 209–220.

Toro, B.A., 1995. Primer hallazgo de graptolitos del Silúrico (Llandoveriano) en la Cordillera Oriental, Provincia de Jujuy, Argentina. Ameghiniana 32, 375–384.

Toro, B.A., 1997. La fauna de graptolitos de la Formación Acoite, en el borde occidental de la Cordillera Oriental Argentina, Análisis bioestratigráfico. Ameghiniana 34 (4), 393–412.

Toro, B.A., Brussa, E.D., 2003. Graptolites, in: Benedetto, J.L. (Ed.), Ordovician fossils of Argentina. Secretaría de Ciencia y Tecnología, Universidad Nacional de Córdoba. pp. 441–505.

Toro, B.A., Maletz, J., 2007. Deflexed *Baltograptus* species in the early to mid Arenig Graptolite Biostratigraphy of northwestern Argentina. Acta Palaeontologica Sinica 46, 489–496.

Toro, B.A., Maletz, J., 2008. The proximal development in *Cymatograptus* (Graptoloidea) from Argentina and its relevance for the early evolution of the Dichograptacea. Journal of Paleontology 82 (5), 974–983.

Toro, B.A., Vento, B.A., 2013. Reevaluación de las Biozonas de *Tetragraptus phyllograptoides* y *T. akzharensis* (Ordovícico Inferior-Floiano) de la Cordillera Oriental Argentina. Ameghiniana 50, 287–297.

Toro, B.A., Meroi Arcerito, F.R., Muñoz, D.F., Waisfeld, B.G., de la Puente, G.S., 2015. Graptolite-trilobite biostratigraphy in the Santa Victoria area, northwestern

Argentina. A key for regional and worldwide correlation of the Lower Ordovician (Tremadocian - Floian). Ameghiniana 52 (5), 535–557.

Toro, B.A., Herrera Sánchez, N.C., 2019. Stratigraphical distribution of the Ordovician graptolite *Azygograptus* Nicholson & Lapworth in the Central Andean Basin (NW Argentina and S Bolivia). Comptes Rendus Palevol 18 (5), 493–507.

Toro, B.A., Heredia, S., Herrera Sánchez, N.C., Moreno, F., 2020. First Middle Ordovician conodont record related to key graptolites from the western Puna, Argentina: Perspectives for an integrated biostratigraphy and correlation of the Central Andean Basin. Andean Geology 47 (1), 144–161.

Turner, J.C.M., 1960. Estratigrafía de la Sierra de Santa Victoria y adyacencias. Boletín de la Academia Nacional de Ciencias 41, 163–196.

Turner, J.C.M., 1964. Descripción Geológica de la Hoja 2c. Santa Victoria, 99.

Turner, J.C.M., Méndez, V., 1975. Geología del sector oriental de los departamentos de Santa Victoria e Iruya, Provincia de Salta, República Argentina. Boletín de la Academia Nacional de Ciencias de Córdoba 51 (1–2), 11–24.

Turner, J.C.M., Mon, R., 1979. Cordillera Oriental, in: Turner, J.C.M (Ed.), Geología Regional Argentina. Academia Nacional de Ciencias, Publicación Especial 1, pp. 57–94.

Vaucher, R., Vaccari, N.E., Balseiro, D., Muñoz, D.F., Dillinger, A., Waisfeld, B.G., Buatois, L.A., 2020. Tectonic controls on late Cambrian-Early Ordovician deposition in Cordillera Oriental (Northwest Argentina). International Journal of Earth Sciences 109, 1897–1920.

Voldman, G.G., Albanesi, G.L., Ortega, G.C., Giuliano, M.E., Monaldi, C.R., 2017. New conodont taxa and biozones from the Lower Ordovician of the Cordillera Oriental, NW Argentina. Geological Journal 52, 394–414.

Waisfeld, B.G., Astini, R.A., 2003. Environmental constraints on faunal patterns. An example in early Ordovician (Arenig) trilobite assemblages from the Argentine Cordillera Oriental, in: Albanesi G.L., Beresi, M., Peralta S.H. (Eds.), Ordovician from the Andes. Serie Correlación Geológica 17, pp. 341–346.

Waisfeld, B.G., Sánchez, T.M. Benedetto, J.L., Carrera, M.G., 2003. Early Ordovician (Arenig) faunal assemblages from western Argentina. Biodiversification trends in different geodynamic and palaeogeographic settings. Palaeogeography, Palaeoclimatology, Palaeoecology 196, 343–373.

Weishauptová, Z., Přibyl, O., Sýkorová, I., René, M., 2017. Effect of the properties of Silurian shales from the Barrandian Basin on their methane sorption potential. Fuel 203, 68–81.

Zimmermann, U., 2011. From fore-arc to foreland: a cross section of the Ordovician in the Central Andes, in: Gutiérrez Marco, J.C., Rábano, I., García-Bellido, D. (Eds.), Ordovician of the World. Cuadernos del Museo Geominero 14, pp. 667–674.

Zimmermann, U., Bahlburg, H., 2003. Provenance analysis and tectonic setting of the Ordovician clastic deposits in the southern Puna basin, NW Argentina. Sedimentology 50, 1079–1104.

FIGURE CAPTIONS

Figure 1. a) Location map of the geomorphological provinces comprised in the Central Andean Basin. **b)** Geological map of the studied area showing sampling localities with conodont and graptolite biostratigraphic control (Modified from González *et al.*, 2003).

Figure 2. Stratigraphic section from the Los Colorados area, Cordillera Oriental (Modified from Astini *et al.*, 2004) showing the position of the samples. **GB:** Graptolite biozone.

Figure 3. Stratigraphic sections from the Argentine Puna showing the position of the samples. **a)** Huaytiquina area, western Puna (Modified from Monteros *et al.*, 1996). **b)** Muñayoc area, eastern Puna (Modified from Martínez *et al.*, 1999). **GB:** Graptolite biozone.

Figure 4. Summary table with the provenance and taxonomy of the graptolite samples.

Figure 5. Photomicrographs of polished fragments of graptolite from the Puna region (Muñayoc section) under reflected plane-polarized light. **(a)** MU-12; **(b)** MU-12; **(c)** MU 9+1 m; **(d)** MU-11; **(e)** MU-11; **(f)** M//U-15. The scale bar is 10 micrometers.

Figure 6. Photomicrographs of polished fragments of graptolite from the Puna region (Muñayoc section) under reflected plane-polarized light. **(a)** MU-11; **(b)** MU-11; **(c)** MU 9+1 m; **(d)** MU-6; **(e)** MU-15; **(f)** MU-15. The scale bar is 10 micrometers.

Figure 7. Photomicrographs of polished fragments of graptolite from the Puna (Huaytiquina section) and Cordillera Oriental (Los Colorados section) regions under reflected plane-polarized light. **(a)** RH-A; **(b)** LC-17; **(c)** LC-17; **(d)** LC-24+40m; **(e)** LC-14; **(f)** LC-17. The scale bar is 10 micrometers.

Figure 8. Histograms of the %GRo measurements of the six samples from the Los Colorados section. **(a)** Sample LC-12; **(b)** Sample LC-14; **(c)** Sample LC-17; **(d)** Sample LC-21; **(e)** Sample LC-24+40m; **(f)** Sample LC-FL.

Figure 9. Thermal maturity modeling of vitrinite reflectance for the Los Colorados section, Cordillera Oriental Argentina using PetroMod 1D Express software. Red stars represent the middle part of the Acoite Formation where the LC-17, LC-21, and LC-24+40m graptolite samples come from.

Table 1. Rock-Eval pyrolysis results

SAMPLES	TOC (%)	Tmax (°C)	S1	S2	HI	PI	OI
CORDILLERA ORIENTAL							
LC-FL	0.22	287	0.66	0.36	161	0.65	88
LC-10+12m	0.50	291	1.88	1.30	258	0.59	63
LC-12	0.23	410	0.51	0.15	65	0.77	150
LC-14	0.40	294	0.99	0.73	185	0.57	119
LC-17	0.25	414	0.36	0.11	43	0.77	160
LC-21	0.15	333	0.12	0.03	17	0.82	187
LC-24+40m	0.23	352	0.43	0.08	33	0.85	155
PUNA							
MU-6	0.68	290	0.23	0.04	6	0.85	31
MU-9+1m	0.90	338	0.11	0.03	3	0.80	57
MU-11	0.81	283	0.57	0.17	20	0.77	21
MU-12	0.63	280	0.43	0.05	8	0.90	49
MU-14	0.72	290	0.96	0.29	40	0.77	16
MU-15	0.67	148	0.31	0.04	6	0.89	26
RH-A	0.09	394	0.14	0.02	26	0.86	500

S1= mg HC/g rock; S2= mg HC/g rock; HI= S2/TOC*100; OI= S3/TOC*100;

PI= S1/(S1+S2)

Nexxys C. Herrera Sánchez: Conceptualization, Formal Analysis, Investigation, Taxonomic Analysis, Biostratigraphic framework, Writing - original draft, Review & Editing; **Blanca A. Toro:** Selection of graptolite samples, Taxonomic Analysis, Biostratigraphic framework, Conceptualization, Formal Analysis, Investigation, Writing - Review & Editing, Funding acquisition; **Ricardo Ruiz-Monroy:** Conceptualization, Formal Analysis, Investigation, Writing - original draft, Review & Editing; **Thomas Gentzis:** Acquisition of data, Investigation, Writing - Review & Editing; **Seare Ocubalidet:** Acquisition of data, Investigation, Writing; **Humberto Carvajal-Ortiz:** Acquisition of data, Investigation.

Declaration of interests

☒ The authors declare that they have no known competing financial interests or personal relationships that could have appeared to influence the work reported in this paper.

☐The authors declare the following financial interests/personal relationships which may be considered as potential competing interests:

Table 2. Graptolite and equivalent vitrinite reflectance, Tpeak and Tpeak-hy

SAMPLES	GRo (%)	Ani GRo (%)*	VRo-eq (%)	Tpeak (°C)	Tpeak-hy (°C)
	CORDILLERA ORIENTAL				
LC-FL	0.78	-	0.73	110	-
LC-10+12m	-	-	-	-	-
LC-12	0.70	-	0.67	103	-
LC-14	0.63	-	0.62	97	-
LC-17	1.11	-	0.97	133	-
LC-21	0.94	-	0.84	122	-
LC-24+40m	0.90	-	0.81	119	-
	PUNA				
MU-6	5.90	10.12	4.47	256	344
MU-9+1m	6.00	8.78	4.54	257	346
MU-11	5.57	8.80	4.23	252	336
MU-12	6.10	9.44	4.61	259	348
MU-14	6.62	10.06	4.99	265	358
MU-15	5.57	9.58	4.23	252	337
RH-A	6.15	ND	4.65	259	349

ND= Not Determined

Ani GRo= Graptolite reflectance in samples with strong anisotropy

*These values were not used for VRo-eq determination and modelling purposes